magnetochemistry

Review

Green Synthesis of Metal and Metal Oxide Nanoparticles: Principles of Green Chemistry and Raw Materials

Liubov Soltys [1], Ostap Olkhovyy [2], Tetiana Tatarchuk [3,4,*] and Mu. Naushad [5,6]

[1] Department of Chemistry, Vasyl Stefanyk Precarpathian National University, 76018 Ivano-Frankivsk, Ukraine; soltys86@gmail.com
[2] Faculty of Pharmacy, Jagiellonian University, Medyczna 9, 30-688 Kraków, Poland; oolkhovyi@gmail.com
[3] Educational and Scientific Center of Material Science and Nanotechnology, Vasyl Stefanyk Precarpathian National University, 76018 Ivano-Frankivsk, Ukraine
[4] School of Science and Technology, Glocal University, Saharanpur 247001, India
[5] Department of Chemistry, College of Science, King Saud University, Riyadh 11451, Saudi Arabia; mnaushad@ksu.edu.sa
[6] Yonsei Frontier Lab, Yonsei University, Seoul 03722, Korea
* Correspondence: tatarchuk.tetyana@gmail.com

Abstract: Increased request for metal and metal oxide nanoparticles nanoparticles has led to their large-scale production using high-energy methods with various toxic solvents. This cause environmental contamination, thus eco-friendly "green" synthesis methods has become necessary. An alternative way to synthesize metal nanoparticles includes using bioresources, such as plants and plant products, bacteria, fungi, yeast, algae, etc. "Green" synthesis has low toxicity, is safe for human health and environment compared to other methods, meaning it is the best approach for obtaining metal and metal oxide nanoparticles. This review reveals 12 principles of "green" chemistry and examples of biological components suitable for "green" synthesis, as well as modern scientific research of eco-friendly synthesis methods of magnetic and metal nanoparticles. Particularly, using extracts of green tea, fruits, roots, leaves, etc., to obtain Fe_3O_4 NPs. The various precursors as egg white (albumen), leaf and fruit extracts, etc., can be used for the „green" synthesis of spinel magnetic NPs. "Green" nanoparticles are being widely used as antimicrobials, photocatalysts and adsorbents. "Green" magnetic nanoparticles demonstrate low toxicity and high biocompatibility, which allows for their biomedical application, especially for targeted drug delivery, contrast imaging and magnetic hyperthermia applications. The synthesis of silver, gold, platinum and palladium nanoparticles using extracts from fungi, red algae, fruits, etc., has been described.

Keywords: green synthesis; magnetite; spinel ferrite; metal nanoparticles

Citation: Soltys, L.; Olkhovyy, O.; Tatarchuk, T.; Naushad, M. Green Synthesis of Metal and Metal Oxide Nanoparticles: Principles of Green Chemistry and Raw Materials. *Magnetochemistry* **2021**, *7*, 145. https://doi.org/10.3390/magnetochemistry7110145

Academic Editors: Vladimir I. Tsifrinovich and Andrea Caneschi

Received: 5 September 2021
Accepted: 27 October 2021
Published: 31 October 2021

1. Introduction

Nowadays, a new page is turning in the history of chemistry, connected with the development of a new integrated scientific direction—"green" chemistry. "Green" chemistry is interdisciplinary: there is an integration of synthetic organic chemistry with analytical chemistry, physical chemistry, toxicology, microbiology, biotechnology and engineering. The goal of "green" chemistry is to develop technologies for more efficient chemical reactions. "Green" chemistry aims to prevent pollution in the very early stages of the planning and implementation of chemical processes and covers all types and aspects of chemical processes to minimize the environmental risks. The problems within the competence of "green" chemistry can be categorized into two main areas. The first relates to the processing and utilization of environmentally hazardous waste and by-products of the chemical industry. The second, more promising, involves the development of new industrial processes to eliminate or minimize the formation and use of harmful products [1]. "Green" chemistry allows to obtain the necessary substance in the safest possible way. It provides the selection of raw materials and process schemes, which generally exclude the use of harmful substances, toxic and hazardous chemicals, and focuses on industrial processes that do not pollute the environment and lay the responsibility for the products on the scientists and manufacturers [2].

As a scientific field, "green" chemistry appeared in the United States in the 1990s. European countries have been implementing the most advanced laws on "green" technologies. In recent years, new reaction schemes and processes have been developed, designed to drastically reduce the burden of chemical production on the environment, to minimize the processing and utilization of hazardous substances and harmful by-products [1]. "Green" chemistry is already moving in three major directions: *new ways of synthesis* (using catalysts); *replacement of traditional organic solvents* (particularly, the use of supercritical CO_2); *renewable source reagents* (i.e., non-petroleum products) [3].

In "green" chemistry, fundamentally new constructs such as "ideal process", "ideal product" and "ideal consumer" are used [4]. The ideal process is a simple, eco-friendly, one-stage process, effective at the molecular level, with the use of renewable raw materials, which provides maximum yield. The ideal product requires a minimum of energy and packaging, is safe, recyclable and fully degradable by microorganisms [1]. Usually the main focus is on the production process and the final product, and the consumer is absent in this scheme. In "green" chemistry, the image of the "ideal consumer" is present—he uses a minimum number of goods, understands the need to preserve the environment. New research frontiers and new terms have been introduced into "green" chemistry: "atom efficiency", "innate safety", "product life cycle analysis", "ionic liquid", "renewable energy", "environmental efficiency", "process intensification and integration", etc.

This review is aimed to analysis of modern scientific research of eco-friendly "green" synthesis methods of magnetic and metal nanoparticles. "Green" nanoparticles are being widely used as antimicrobials, photocatalysts and adsorbents [5–7]. "Green" magnetic nanoparticles demonstrate low toxicity and high biocompatibility, which allows their biomedical application, especially for targeted drug delivery, contrast imaging and magnetic hyperthermia applications. The structure and morphology of synthesized magnetic nanoparticles can be characterized by scanning electron microscopy, transmission electron microscopy, energy-dispersive analysis, X-ray diffraction analysis, X-ray photoelectron spectroscopy, FTIR spectroscopy, Raman spectroscopy and magnetic force microscopy. Magnetic force microscopy (MFM) is a scatter-sensitive technique with a resolution of up to 10 nm that can detect weak magnetic fields. MFM is a universal method of analysis of magnetic nanoparticles due to the simple requirements for sample preparation, the ability to work in air, vacuum or liquid medium [8]. Due to this, MFM is a powerful tool for imaging of magnetic NPs, characterizing their size and morphology. For superparamagnetic nanoparticles, MFM has been especially useful to evaluate magnetic moment, magnetic anisotropy, magnetization curves and the effect of aggregation in particles [9]. The ability of MFM to detect superparamagnetic and low-coercive magnetic nanoparticles and the interpretation of the obtained MFM images are the subject of many research [10–15]. Torre et al. [10] demonstrated the ability of magnetic force microscopy (MFM) to quantify magnetic textures at room temperature. MFM measurements were performed for magnetic nanoparticles of iron oxide with a diameter of 11 nm. The obtained images of nanofilms, which were applied to the substrate, indicated linear magnetic chains of nanoparticles of several hundred nanometers. In a study [11] the authors quantified the magnetization of individual magnetic NPs using MFM. Cordova et al. [12] used MFM to analyze the superparamagnetic iron oxide NPs in air, liquid medium and inside thin polymer films. The authors of work [13] used MFM to analyze the magnetite NPs with different sizes (from 10 nm to 100 nm), which are embedded in polymer films with different thickness. Therefore, MFM allows to quantify the magnetic properties of both single nanoparticles and nanoparticles in non-magnetic matrices (e.g., polymers).

2. The Principles of "Green" Chemistry

In 1998 Paul Anastas and John Warner in their book "Green Chemistry: Theory and Practice", Ref. [2] formulated 12 principles of "green" chemistry. They recommend the scientists, industrialists and government officials to direct their activities to reduce or eliminate the use of hazardous materials and chemical processes. These 12 principles, due to their relevance, usefulness and specificity, have made a significant contribution to the expansion and formation of a new philosophy.

The ***principles*** are following (Figure 1):

- *prevention of waste* (chemical synthesis design that prevents waste rather than its disposal or utilization);
- *maximum increase of components—"atom economy"* (design of synthesis to maximize raw materials ratio in the final product with the least or no amount of waste);
- *development of less dangerous chemical syntheses* (generating and using substances with minimal or zero toxicity);
- *design of safe chemicals and products* (chemicals that are effective yet non-toxic);
- *use of safe solvents and reaction conditions* (minimize or exclude the use of solvents or other auxiliary chemicals, and if necessary—use the safest of them);
- *increase energy efficiency* (identify and minimize the consequences caused by using energy in chemical synthesis. Initiate chemical reactions at room temperature and pressure, if possible);
- *use of renewable raw materials* (sources of renewable raw materials are agricultural products or waste);
- *avoidance of chemical derivatives* (minimize or eliminate the use of blocking or protective groups or any temporary modifications, if possible);
- *use of non-stoichiometric catalysts* (minimization of waste by implementation of catalytic reactions, use of effective catalysts in small quantities that can promote the reaction repeatedly);
- *design of degradable chemicals and products* (non-persistent, which decompose into safe substances);
- *real-time analysis of pollution* (elimination or minimization of by-products through interfering with the process during synthesis);
- *minimizing the possibility of accidents* (such as releases, explosions and fires) through designing safer chemicals and their physical forms (solid, liquid or gaseous).

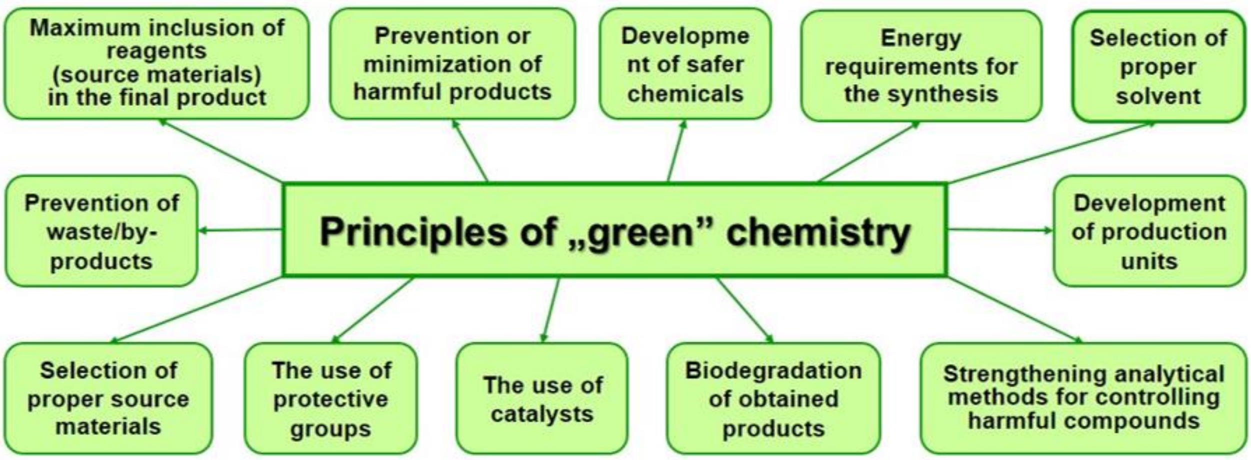

Figure 1. Principles of "green" chemistry.

R.A. Bourne et al. [3] presents 12 principles of "green" chemistry using the abbreviation "PRODUCTIVELY" (Figure 2). Let us look closely to each of the 12 principles [16,17].

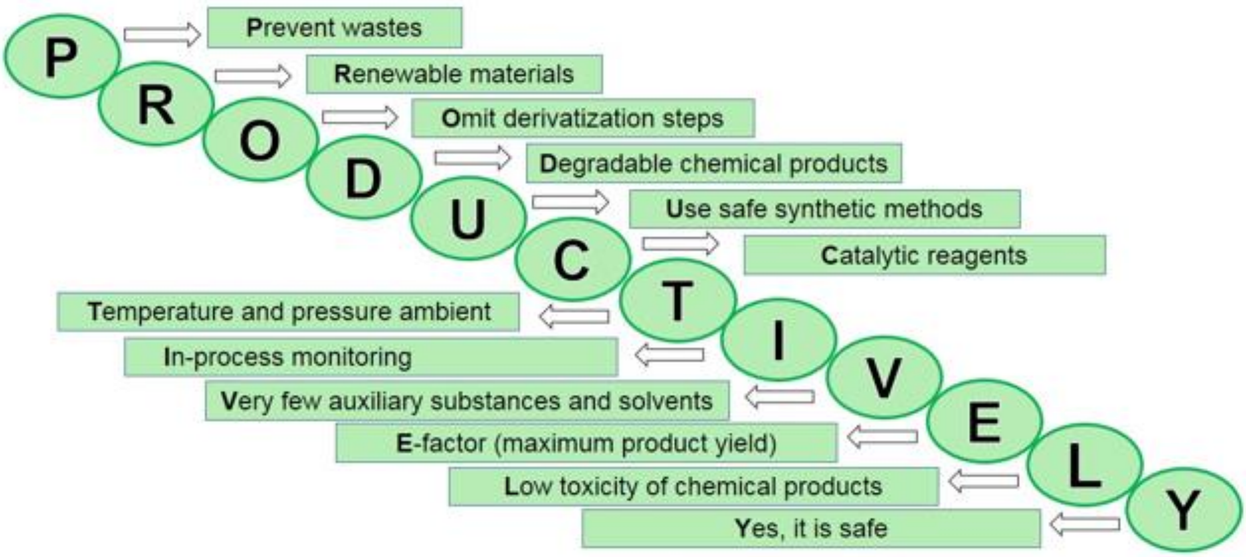

Figure 2. The principles of "green" chemistry.

2.1. Prevention (Reducing) of Waste/by-Products

The major principle is called the prevention principle, and the other principles are the "how-to's" to achieve it. The best way is to carry out the synthesis with zero or no waste (by-products), because the costs associated with the waste disposal significantly increase the total cost of production. Even unreacted raw materials are part of the waste. Therefore, we should avoid the generation of waste (or by-products), which causes pollution when dumped into the atmosphere, sea or land and requires cleaning costs [16]. Introduction of the E-factor ("by-products/final product" ratio) by Roger Sheldon of Delft University (the Netherlands) was an important innovation of "green" chemistry. It characterizes the loss per 1 kg of target product, allows to compare chemical production technologies, and is crucial for attracting attention of global chemical and pharmaceutical industries to the issue of waste [18].

2.2. Maximum Inclusion of Reagents (Source Materials) in the Final Product

When one mole of reagent results in one mole of product, the yield is 100%. Chemists around the world consider the reaction quite effective, when the yield is about 90%. However, product yield calculations can create excessive waste (or by-products). Typical examples, such as the Grignard or Wittig reactions, confirm those statement. Aforementioned reactions can result in 100% yield, but ignore the number of by-products. The reaction is considered "green" if there is a maximal inclusion of precursors in the final product [16].

The term "atom economy" was introduced in 1973 and has become a basic concept among researchers in this field of chemistry. The main goal of atom economy was to overpass the limitations of traditional "profitability", the amount of final products used in calculating the effectiveness of reactions. For example, to calculate yields, chemists considered the effectiveness and amount of just the basic chemical product they chose ("target molecules"), excluding possibly hazardous by-products. The atom economy takes into account all the components and reagents of the reactions, thus providing a reliable indicator of whether pollutants are formed during the reaction. Green chemistry has proven the reduction of pollution to be possible through atom economy, which relies on such processes as hydrogenation, metathesis and cycloaddition.

2.3. Prevention or Minimization of Harmful Products

"Green" chemisty's major principle is to avoid or reduce the formation of hazardous products. The danger to workers can be decreased by using protective clothing, respirators, etc. This, however, increases the cost of production. To avoid risks, "green" chemistry has found a scientific solution to such situations [16].

2.4. Development of Safer Chemicals

A priority is to ensure that the synthesized chemicals (dyes, paints, adhesives, cosmetics, pharmaceuticals, etc.) are harmless. An example of a dangerous substance is thalidomide (introduced in 1961) for nausea and vomiting of pregnancy. Has been proven that the children born to women taking this drug had different birth defects (including missing or deformed limbs). Subsequently, thalidomide was banned and strict rules for testing new drugs were implemented. With the development of technology, it has become possible to produce safer chemicals by manipulating the molecular structure of substances [16].

2.5. Energy Requirements for the Chemical Synthesis

The minimum energy requirement must be adhered to any chemical processes. For instance, if the precursors are soluble in a specific solvent, the reaction mixture must be heated for some time or until completion. In such sircumstance, the time required to complete the reaction should be minimal with a minimum amount of energy required. A catalyst can be used to reduce the energy needs of the reaction. In case of an exothermic reaction, large cooling is sometimes required. Sometimes the final product must be purified by ultrafiltration, distillation, or recrystallization. All these stages are energy consuming and increase the total cost. Final energy requirements can be minimal if the process is planned so that there is no need for separation or purification [16].

2.6. Selection of Proper Solvent

The chosen solvent should not lead to any environmental contaminations or health hazards. The use of liquid or supercritical CO_2 should be studied. If possible, the reaction should be performed in the water medium or without a solvent. The best method is to perform the reaction in the solid phase. One of the main problems with many solvents is their volatility, which can be harmful to the health and ecosystems. In order to avoid this, immobilized solvents can be used. They maintain the solubility of the material, are non-volatile and safe. Immobilization can be carried out by attaching the solid substances to a solid phase or by binding the solvent molecule directly to the polymer matrix. Several newly discovered polymeric substances as solvents have been found to be non-hazardous [16].

2.7. Selection of Proper Source Materials

Source materials are derived from renewable or non-renewable materials. Petrochemicals are usually derived from crude oil, that is not a renewable source. Raw materials obtained from agricultural or organic products are called renewable. However, such factors as crop failure, etc., may interfere with constant supply of agricultural products. Substances such as carbon dioxide (formed naturally or synthetically) and methane (derived from natural sources) are in sufficient quantities. They are considered as renewable raw sources [16].

2.8. The Use of Catalysts

Catalysts promote the reaction without being consumed and included in the final product. Thus, they should be used whenever possible. The benefits of catalysts include: (i) better product yield; (ii) the reaction becomes possible in cases where it does not occur normally; (iii) increased selectivity. In addition, the use of catalysts has significant advantages in energy demand, better utilization of raw materials and waste minimization. With advances in the catalysts selectivity, certain "green" synthesis reactions have become very convenient [16].

2.9. Biodegradation of Obtained Products

The problem of non-biodegradable products is especially common with insecticides and polymers. Farmers are using different types of insecticides in order to protect crops from insects. Widely used insecticides include less stable (carbamates, organophosphates) and more stable (chlorinated hydrocarbons). Although the latter are certainly effective, they are usually bioaccumulated in flora and fauna and included in the food chain. The insecticides cause a decrease in the population of beneficial insects and animals (honey bees, butterflies, mites, etc.). Given the above, it is crucial that any synthesized product is biodegradable and non-toxic [16].

2.10. Strengthening Analytical Methods for Controlling Harmful Compounds

Analytical methods should be designed to require minimal use of chemicals. For example, processing some unreacted chemicals to complete the reaction. It is also useful to place sensors to track the formation of toxic by-products during a chemical process [16].

2.11. Development of Production Units

The importance of accident prevention in production units cannot be overstated. A number of industrial accidents have occured and caused not only in the loss of thousands of lives but also in lifelong disabilities. Production facilities should be fabricated to exclude the accidents possibility caused by toxicity, explosions, fires, etc., during operation [16]. Many industrial enterprises have welcomed the proposed 12 principles and have made some progress in improving the safety of their chemical plants. For example, the world-famous company Pfizer has developed a new technology for the production of sildenafil citrate. While the old technology required 1300 L of solvent containing chlorine, the new—only 6.5 L of safe solvent. As a result, the mentioned E-factor of such production decreased from 105 to 6, and the pharmaceutical giant itself received a prize from the British government [3].

3. Raw Materials for "Green" Chemistry

3.1. Transition to Renewable Raw Materials

During last 80 years, the chemical industry has been based on natural gas and crude oil as the main raw sources. However, today there is a trend towards transition from fossil to renewable raw resources, such as carbohydrates and biomass-derived triglycerides [18]. A partial transition to renewable energy sources is desirable for such reasons as biocompatibility, biodegradability and lesser toxicity. Products based on renewable raw materials are obtained from carbon dioxide and water via photosynthesis and after being used, are eventually returned to the biosphere as CO_2 and H_2O through biodegradation. They are becoming more reliable and cheaper compared to the rapidly increasing gas and oil prices. The developing of "green" products, which can replace petroleum-based products and the implementing of «green synthesis» methods for the chemicals production from biomass, are the main in the transition to renewable raw materials. For example, the catalysts (like modified corn starch with surface -SO_3H/-NH_2 groups) for chemical reactions can be obtained from biomass [18,19].

3.2. Biological Components for "Green" Synthesis

In order to obtain "green" nanoparticles with required shape, size, and properties, two synthesis principles are being considered: "top-down" and "bottom-up" [20]. In the "bottom-up" approach, the NPs are formed first, and then assembled into the final material. The benefit of the „bottom-up" principle is the opportunity of obtaining small metal NPs with uniform chemical composition. In the „top-down" approach, the source material is reduced in size by physical (e.g., mechanical) or chemical methods. The main disadvantage of this approach is the defects of the material surface, which can significantly affect the properties of metal nanoparticles [21].

The environmentally friendly and sustainable synthesis methods are using in "green" chemistry in order to prevent the formation of toxic by-products [22–24]. Different biological materials, such as plant extracts, algae, fungi, bacteria, etc., are used in the "green" synthesis of metal and metal oxide NPs [25–36]. The use of plant extracts is fairly easy for obtaining NPs on a large scale, compared to the synthesis with fungi and bacteria [20,37,38].

Various factors (pH, pressure, temperature, solvent type) affect the "green" synthesis techniques. However, the key role is belongs to the phytochemicals, which are presented in plant extracts (roots, leaves, stems, fruits): ascorbic acids, phenols, carboxylic acids, terpenoids, amides, flavones, aldehydes, ketones etc. [39–42]. These components reduce metal salts to metal NPs [20]. There are different mechanisms of NPs formation using microorganisms [38]. A huge variety of nature biological materials, including plants [43–51], algae [52–56], fungi [57–61], yeast [62–65], bacteria [66–69], viruses [70], etc., can be used for the synthesis of "green" NPs (Figure 3).

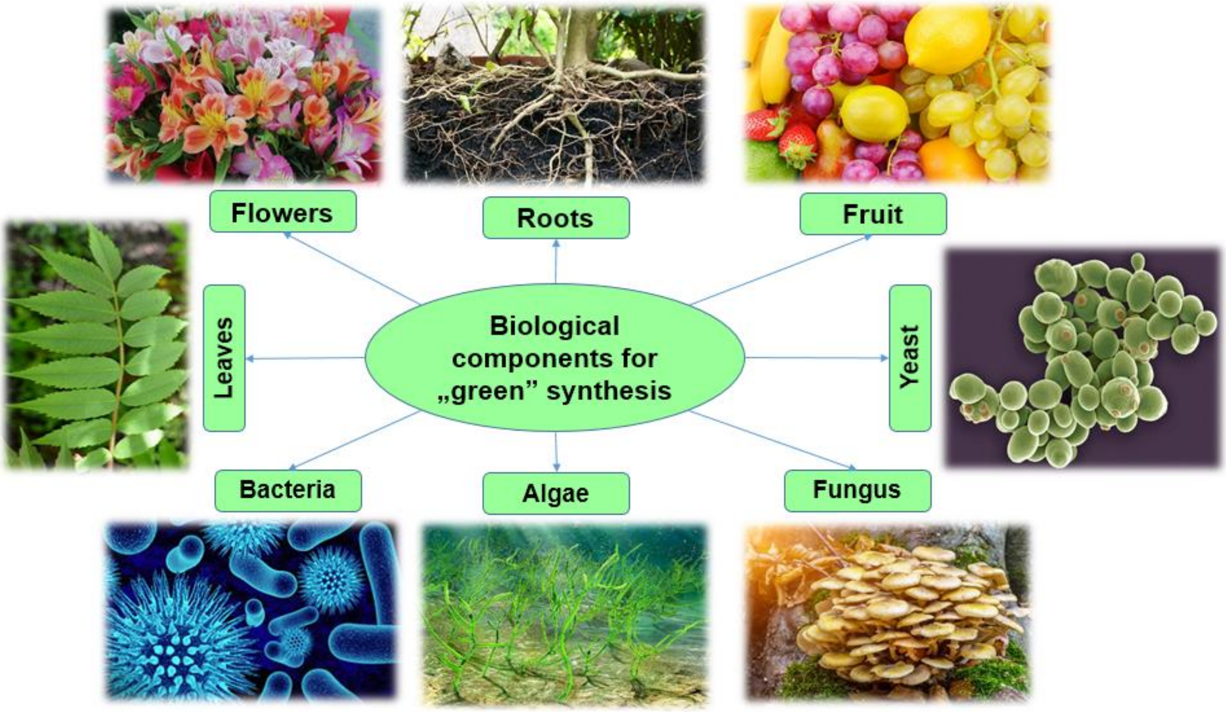

Figure 3. Various natural resources used for the synthesis of "green" nanoparticles.

3.2.1. Bacteria

Bacteria are widely used for genetic engineering, bioremediation and bioextraction. Various types of bacteria are able to reduce metal ions and are important in NPs obtaining. In particular, prokaryotic bacteria and actinomycetes are widely used for the synthesis of metal or metal oxide NPs [20]. Some examples of bacterial strains that are widely used for the obtaining of bio-reduced silver NPs with different size and morphologies include: *Shewanella oneidensis*, *Arthrobacter gangotriensis*, *Enterobacter cloacae*, *Bacillus cecembensis*, *Bacillus indicus*, *Bacillus amyloliquefaciens*, *Bacillus cereus*, *Lactobacillus casei*, *Escherichia coli*. For the synthesis of AuNPs, the following bacteria are used: *Plectonema boryanum* UTEX 485, *Rhodopseudomonas capsulate*, *Shewanella alga*, *Bacillus subtilis* 168, *Desulfovibrio desulfuricans*, *Bacillus megaterium* D01 [21].

3.2.2. Fungi

Fungus-mediated metal/metal oxide NPs biosynthesis is also very productive for obtaining monodisperse NPs with desired morphologies. They are preferable for the production of metal and metal oxide NPs because of various intracellular enzymes. Proper fungi can synthesize more nanoparticles than bacteria. Furthemore, the presence of reducing components, enzymes, proteins in their cells grants them advantage over other organisms. The probable mechanism of metal nanoparticle formation is an enzymatic reduction (reductase) in the cell wall or inside the fungal cell [20]. A clear advantage of fungi in the synthesis of nanoparticles is the simplicity of their scaling (e.g., using the method of thin solid substrate fermentation). The fungi are highly effective secretors of extracellular enzymes. Thus, it is easy to obtain large-scale production of enzymes. More advantages of using fungi in the "green" synthesis of metal nanoparticles include economic viability and easy biomass handling. However, there is a significant disadvantage of using these bioformations in the synthesis of nanoparticles as the genetic manipulation of eukaryotes is much more complex than prokaryotes [21].

3.2.3. Yeast

Yeast is a unicellular microorganism that is present in eukaryotic cells. Only 1500 species of yeast have been identified. Numerous research groups have reported the successful synthesis of nanoparticles/nanomaterials using yeast. Many different types are used to produce countless metal nanoparticles [20,62].

3.2.4. Plants

Plants can accumulate heavy metals in leaves, roots, fruits, etc. Therefore, synthesis using plant extracts attract attention as simple, effective, cheap and feasible methods for obtaining nanoparticles [71–73]. Various plants can be used for reduction and stabilization of metal nanoparticles during synthesis. Many researchers use "green" synthesis to obtain metal oxide NPs using plant extracts for varius applications [74–78]. The plant extracts are mixed with the solutions of metal precursors under different reaction conditions [79–82]. Such parameters as temperature, pH, metal salt concentration, types and concentration of phytochemicals affect the stability and the rate of NPs formation. Biologically active compounds found in plants (Figure 4) due to the presence of functional groups are able to reduce metal ions much faster than bacteria or fungi. Amides, carboxylic acids, aldehydes, ketones, sugars, terpenoids and flavones are among essential phytochemicals, which are responsible for the NPs bioreduction [83–86].

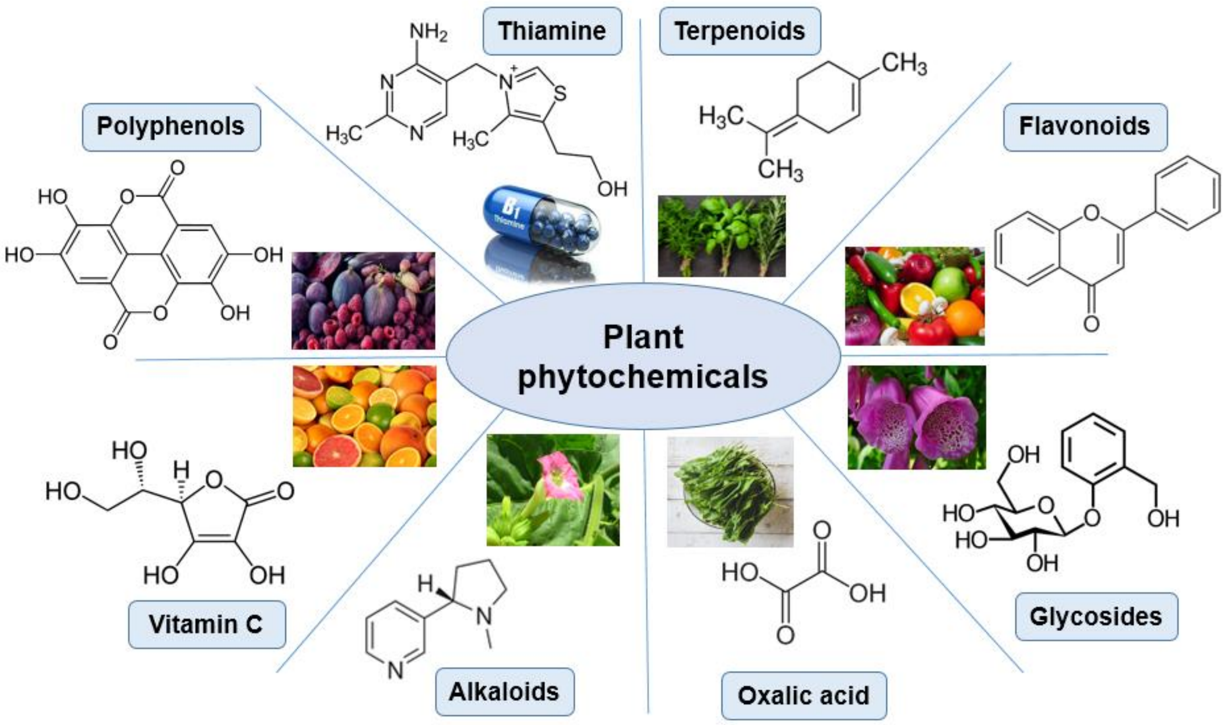

Figure 4. Plant phytochemicals.

Plants contain biologically active compounds (carbohydrates, coenzymes and proteins) with excellent ability for the reduction of metal salts to NPs [87,88]. The syntheses of gold [89–94] and silver [95–101] nanoparticles involving plant extracts were the first to be studied. Various plants are used: lemon grass (*Cymbopogon flexuosus*), mustard (*Brassica juncea*), coriander (*Coriandrum sativum*), grape (Vitis), Ginkgo Biloba, Cydonia oblonga, neem (*Azadirachta indica*), lemon (*Citrus limon*), tulsi (*Ocimum sanctum*), oats (*Avena sativa*) and aloe vera (*Aloe barbadensis*). The Zn, Ni, Co and Cu NPs is obtained using sunflower (*Helianthus annuus*), alfalfa (*Medicago sativa*) and mustard (*Brassica juncea*). ZnO NPs were also obtained from a wide number of plant extracts, such as green tea (*Camellia sinensis*), China rose (*Hibiscus rosa-sinensis*), copperleaf (*Acalypha indica*), coriander (*Coriandrum sativum*) and crown flower (*Calotropis gigantea*) [20,102–104].

3.3. Solvent-Based "Green" Synthesis"

Solvent systems are the main components in the synthesis process. Most common solvents are harmful. One of the well-known solvents is benzene, which causes cancer in humans. Some of the aromatic solvents, such as toluene, can cause brain damage, affect speech, vision, and cause problems with kidney. Halogen-containing solvents, such as dichloromethane, carbon tetrachloride, perchloroethylene and chloroform, are also commonly used and having been recognized as carcinogens [16].

Water is an ideal solvent, as it is the cheapest and most available, and has been used in the synthesis of various nanoparticles since the beginning of nanoscience and nanotechnology [20]. ***Carbon dioxide*** is a universal solvent, which is used as liquid CO_2 or supercritical CO_2. The gas usually turns into a liquid state after increased pressure. However, if the CO_2 is put at a temperature above 31 °C and at a supercritical pressure equal 7.38 kPa, a supercritical liquid is formed [16]. ***Supercritical*** and ***ionic liquids*** are some of the best solvents applied in „green" synthesis. Ionic liquids consist of ions with melting points below 100 °C. They are called „ionic liquids at room temperature". The ability of ionic liquids to be both reducing and protective agents simplifies the process of nanoparticle synthesis. Ionic liquids can be hydrophilic or hydrophobic based on the anions and cations nature [20]. The advantages of using ionic liquids as solvents are: (i) easy solubility of many organic compounds, metals and gases in ionic liquids; (ii) constructive thermal stability when operating in a wide temperature range (ionic liquids have a 3–4 times larger temperature range of synthesis, compared with water); (iii) ionic liquids do not coordinate, compared to other polar solvents or alcohols; (iv) ionic liquids do not evaporate as volatile organic solvents; (v) ionic liquids are amphilites due to the presence of cations and anions [20]. However, the main disadvantage of ionic liquids is their non-biodegradability. Thus the new ionic liquids with high biodegradation efficiency are being developed.

4. "Green" Synthesis and the Use of Magnetic Nanoparticles

4.1. Effect of Magnetic Nanoparticles on Environmental Restoration

In recent years, the environment has been polluted due to the excessive use of fertilizers and pesticides [105–108]. Extensive research work is underway to study various aspects of environmental restoration using magnetic nanoparticles, which includes cleaning the atmosphere, soil, sedimentary rocks, groundwater and surface water [109]. The synthesis of magnetic nanoparticles is the subject of number of systematic research related to their technological applications [110]. Magnetic nanoparticles have demonstrate high potential in environmental and biomedical applications [109,111,112]. Magnetic NPs are able to detoxify the environment due to the high specific surface area. They act as a "superabsorbent" for many contaminants, converting them into non-toxic forms. Magnetic nanoparticles are usually consists from Fe, Ni, Co or their oxides, such as magnetite (Fe_3O_4), maghemite (γ-Fe_2O_3), cobalt ferrite ($CoFe_2O_4$) etc. They can be controlled by magnetic fields [109]. The earliest reports of the synthesis of magnetic iron oxide particles, which form relatively stable colloids, date back to the 1930s. The first stable suspension of magnetic particles was obtained in 1965 by Steve Papell. His magnetic fluid was a dispersion of crushed particles of magnetite (Fe_3O_4) (diameter <25 mm) modified with oleic acid. These particles were dispersed in non-polar solvents (carrier), forming a stable magnetic fluid, which was used to give the fuel its magnetic properties. Rosensweig obtained several types of magnetic fluids based on the dispersion of crushed Fe_3O_4 particles in various carriers, such as kerosene, water, fluorocarbons and esters. In 1982, Massart obtained magnetic fluids by chemical means, which involved the co-precipitation of Fe(II) and Fe(III) hydroxides, and modified the co-precipitation method to obtain ultrastable and highly concentrated magnetic fluids with different magnetic particles based on spinel ferrites, such as $(M_{1-x}{}^{2+}Fe_x{}^{3+})_A[Fe_{2-x}{}^{3+}M_x{}^{2+}]_BO_4$ (M = Mn, Co, Ni, Cu, Zn). The stability of such dispersions is achieved via hydrothermal treatment of samples with $Fe(NO_3)_3$, which leads to the formation of a protective layer rich in iron, which passivates the nanoparticle surface [110]. However, these techniques do not allow good control of the nanoparticles morphology. Therefore, the researchers' efforts were focused on finding ways of synthesis where better control of the size and shape of magnetic nanoparticles can be achieved. Many scientific studies present different concepts for controlling the morphology of synthesized magnetic nanoparticles, but none of them fully meet all the principles of "green" chemistry [110]. There are several types of magnetic nanoparticles: ferrites, core-shell NPs (magnetic core plus shell from SiO_2, for example), metal NPs (are pyrophoric and react to oxidants, what complicates their use and causes undesired side effects) etc. [113]. Magnetic NPs, coated with SiO_2, have a few advantages over metal nanoparticles: higher chemical stability; narrow size distribution; higher colloidal stability; adjustable magnetic moment by the size of the nanoparticle cluster; preserved superparamagnetic properties; the SiO_2 surface allows direct covalent functionalization [113].

4.2. Superparamagnetic Iron Oxide (Magnetite) Nanoparticles and Their Application

Magnetite Fe_3O_4 is a most common natural iron oxide with inverse spinel structure. The ferrous (Fe^{2+}) ions occupy half of the octahedral positions of Fe_3O_4 spinel structure due to the higher field stabilization energy of black crystalline substances, and Fe^{3+} occupy the remaining octahedral positions and all tetrahedral positions. The magnetic behavior of Fe_3O_4 nanoparticles strongly relies on the synthesis method. In addition, the NPs morphology are key to magnetic properties of magnetite. Therefore, for better application, it is necessary to determine the optimal parameters of Fe_3O_4 nanoparticles [114].

Superparamagnetic Fe_3O_4 NPs are well known due to their unique properties: biodegradability, biocompatiblity and non-toxic effect. If the nanoparticle size less than 50 nm in diameter, they are suitable for effective endocytosis with the use of drugs. Therefore, many synthesis methods (co-precipitation method, sol-gel method, hydrothermal synthesis, solid-state synthesis, flame spraying synthesis, thermal decomposition, solvothermal synthesis, etc.) to obtain Fe_3O_4 nanoparticles with the desired properties have been reported [114]. Figure 5 shows the possible use of Fe_3O_4 nanoparticles, namely: as a catalyst, for water purification (removal of heavy metal ions), lithium-ion batteries, biomedical applications, tissue engineering etc. All these studies show promising results and provide a platform for Fe_3O_4 nanoparticles, whose unique features provide great potential for their widespread use.

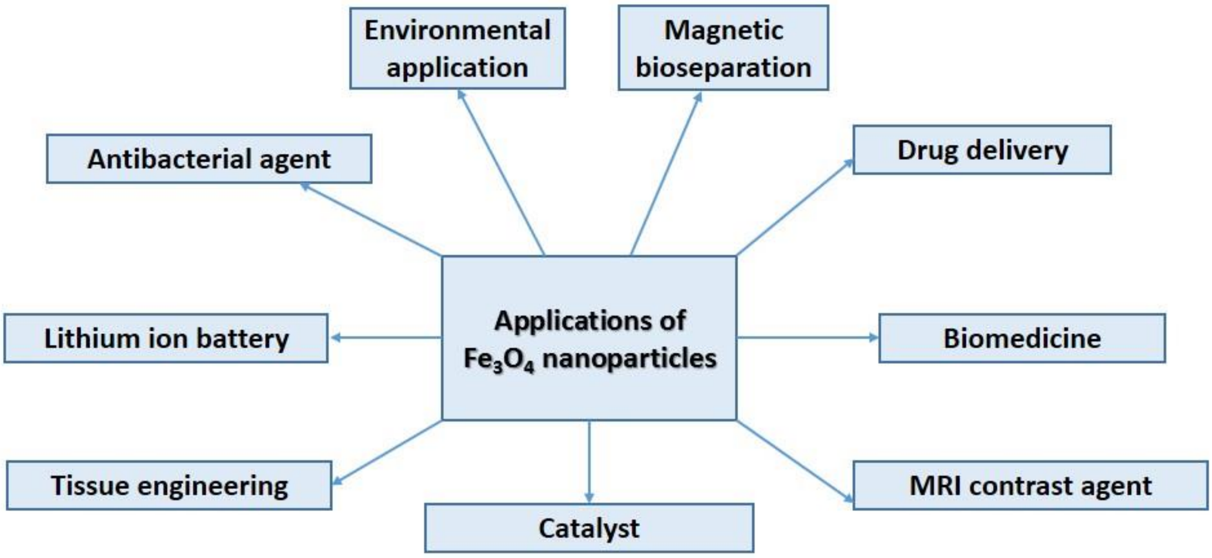

Figure 5. Applications of magnetite nanoparticles.

Maghemite (γ-Fe_2O_3) is isostructural with magnetite, but it has cation vacancies and quite similar general properties, even though maghemite is generally less magnetic but more stable than magnetite. It can be obtained by direct oxidation of magnetite. Although maghemite does not always need a shell for stabilization or a graft to the surface with polymers (such as polyethylene glycol), they are often used in the biological system and increase the half-life of nanoparticles in the blood. The increase in half-life is usually associated with a delay in the opsonization process, in which particles are targeted by phagocytic immune cells, resulting in rapid clearance to the liver or spleen through the reticuloendothelial system. Another way to increase the half-life is to add a biomolecular corona that interacts with biological systems. This corona can be the main element of the biological identity of the nanoparticle [115].

The "green" synthesis of magnetic nanoparticles uses a "bottom-up" approach, when metal atoms gather and form clusters, and then NPs [116–124]. Biologically active substances, which are presented in "green" sources, can reduce and stabilize nanoparticles during synthesis. This allows to control their shape and morphology required for specific applications [114,125–129].

4.3. "Green" Synthesis of Magnetic Fe_3O_4 Nanoparticles

Here are some examples of using "green" synthesis to obtain magnetic Fe_3O_4 nanoparticles, and their practical application (Figure 6). Venkateswarlu et al. [130] reported a removal of Pb(II) using DMSA-modified Fe_3O_4 (DMSA = dimercaptosuccinic acid). Fe_3O_4 were obtained by "green" method using *Punica Granatum* peel extract from $FeCl_3{\cdot}6H_2O$ and CH_3COONa precursors. Then, 0.926 g of dried product (Fe_3O_4) and 0.7288 g of DMSA were added to 40 mL of double distilled water, mixed together with ultrasound for 10 h at room temperature, and the pH was adjusted to 8 by adding 0.01M NaOH solution dropwise. After 10-h reaction, the obtained DMSA@Fe_3O_4 were separated under an external magnetic field, washed and dried at 90 °C in vacuum. These magnetic DMSA@Fe_3O_4 nanorods were used to remove Pb(II) from water medium. The adsorption capacity was equal to 46.18 mg/g at a dosage of 0.1 g/L and T = 301 K. The experimental data corresponded to the kinetic model of the pseudo-second order. Figure 6a shows the magnetic properties DMSA@Fe_3O_4 magnetic nanorods (MNRs) and Figure 6b shows TEM image of Fe_3O_4 and DMSA@Fe_3O_4 MNRs. The results indicate that the synthesized biogenic DMSA@Fe_3O_4 nanorods could be used as promised adsorbent for the Pb(II) removal.

Niraimathee et al. [131] obtained iron oxide NPs using iron sulfate ($FeSO_4 \cdot 7H_2O$) and an aqueous extract of *Mimosa pudica* root containing mimosin, which acts as a reductant. IR spectroscopy approved the presence of biologically active plant molecules on the iron oxide NPs surfaces. The obtained iron oxide NPs can be used directly in the targeted delivery of pharmaceuticals.

Lunge et al. [132] successfully synthesized magnetic Fe_3O_4 NPs (MION-Tea) using tea waste as green reductant. MION-Tea exhibited supermagnetic nature (Figure 6c) and reveals the cuboidal/pyramidal shaped structure of Fe_3O_4 (magnetite) crystals. TEM analysis of MION-Tea shows that the formed NPs are in the range of 5–25 nm (Figure 6d). MION-Tea NPs were investigated as adsorbents for As(III) and As(V) removal from water medium. The adsorption capacity was 188.69 mg/g for As(III) and 153.8 mg/g for As(V). Comparison with known adsorbents revealed that MION-Tea has potential for the As(III) and As(V) ions removal.

Bahadur et al. [133] performed a detailed examination of the optical, thermal, magnetic and dielectric properties of citric acid modified superparamagnetic Fe_3O_4 NPs (Cit-USPMNs), obtained via a "green" co-precipitation route. Lemon juice was used as a source of citric acid. Cit-USPMNs were superparamagnetic with low coercivity and saturation magnetization from 31.4 emu/g to 61.8 emu/g (Figure 6e). The size of Cit-USPMNs was in the range of 11–15 nm (Figure 6f).

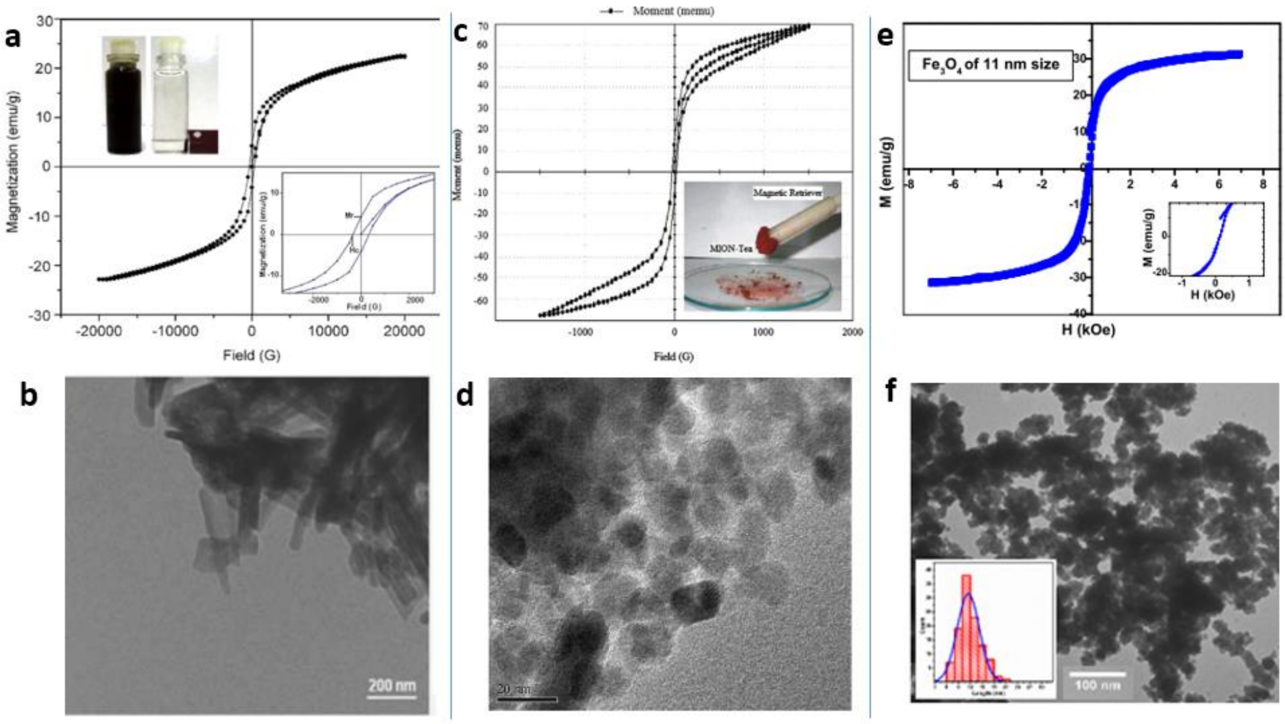

Figure 6. (**a**) VSM of DMSA@Fe_3O_4 MNRs. Upper inset shows DMSA@Fe_3O_4 MNRs dispersed in water and its magnetic separation and lower inset shows the enlargement of the hysteresis loop at low magnetic field (Adapted with permission from [130], Elsevier, 2019); (**b**) TEM image pattern of DMSA@Fe_3O_4 MNRs (Adapted with permission from [130], Elsevier, 2019); (**c**) VSM Magnetization curve of MION-Tea (insight nanoparticles attracted by magnetic retriever) (Adapted with permission from [132], Elsevier, 2014); (**d**) TEM image of MION-Tea (Adapted with permission from [132], Elsevier, 2014); (**e**) M-H loop for Cit-USPMNs (11nm) at room temperature (Adapted with permission from [133], Elsevier, 2017); (**f**) TEM image of Cit-USPMNs (11nm) (Adapted with permission from [133], Elsevier, 2017).

Kanagasubbulakshmi et al. [134] revealed that the *Lagenaria siceraria* leaf extract is suitable for "green" synthesis of magnetite nanoparticles with enhanced antimicrobial properties. The synthesized Fe_3O_4-NPs were of cubic shape and the size range from 30 to 100 nm. Phytochemicals, which are presented in the leaves, act as reducing agents.

The –OH and –COOH functional groups present in nanoparticles make them hydrophilic, so they do not require additional functional modification. The antimicrobial properties of the "green" Fe_3O_4-NPs were investigated against gram-negative (*E. coli*) and gram-positive (*S. aureus*) bacteria strains. It was concluded that "green" Fe_3O_4-NPs demonstate great potential for biomedical applications.

Padhi et al. [135] reported a new single-stage hydrothermal synthesis of photocatalytically stable and magnetically separated g-Fe_3O_4/2RGO nanocomposite in the presence of *Averrhoa carambola* leaf extract (as a natural surfactant for multipurpose use) for water purification. The adopted hydrothermal process leads to good incorporation of g-Fe_3O_4 nanoparticles with an average size of 22 ± 2 nm into 2D sheets of graphene oxide (RGO). *Averrhoa carambola* leaf extract was crucial in modifying the structural, optical and electronic properties of Fe_3O_4 nanoparticles. At room temperature, the g-Fe_3O_4/2RGO nanocomposite showed 97% in Cr(VI) reduction (50 mg/L in 1 h) and 76% in phenol degradation (10 mg/L in 2 h) under visible light. A higher activity of g-Fe_3O_4/2RGO is due to the presence of RGO *in situ*, which led to better separation of photoexcited charge carriers (e^-/h^+). In addition, g-Fe_3O_4/2RGO nanocomposite exhibited better antimicrobial activity against three bacterial pathogens, such as *Staphylococcus aureous* (MTCC-737), *Bacillus subtilis* (MTCC-736) and *Escherichia Coli* (MTCC-443), compared to GO and standard antibiotics (30 μg). The study proves g-Fe_3O_4/2RGO nanocomposite to be potentially useful as a good antibacterial agent.

Kataria et al. [136] synthesized new biogenic "green" magnetic iron oxide NPs, loaded with sawdust carbon (SC) and functionalized with EDTA (EDTA@Fe_3O_4/SC), to remove Cd(II) from the aqueous medium. The adsorption capacity toward Cd(II) ions was 63.3 mg/g. The results of regeneration studies proved the modified EDTA@Fe_3O_4/SC to be promising, cheap and eco-friendly for the adsorption of heavy metals from water environment.

Ahmadian-Fard-Fini et al. [137] prepared the Fe_3O_4/carbon dots nanocomposite for *E.coli* bacteria detection. Carbon dots (CDs) were obtained via hydrothermal method using extracts of grapes, lemon and turmeric in the presence of ethylenediamine. Next, Fe_3O_4 (magnetite) nanoparticles were obtained using these biocompatible retaining reagents. Figure 7a shows VSM curve of Fe_3O_4-carbon dot nanocomposite, and Figure 7b shows TEM image of magnetite-carbon dot core-shell nanocomposite. The results reveal the quenching of the photoluminescence of nanocomposites by increasing the number of bacteria.

Nnadozie et al. [138] reported a "green" biosynthetic co-precipitation of magnetite nanoparticles using *Chromolaena odorata* root extract, which acted as a precipitator and binder for nanoparticles. The extracted phenolic plant component was alkalized with 28% aqueous ammonia solution to pH 13, and added while stirring into the precursor solution (Fe^{2+} and Fe^{3+} ions in a 1:2 molar ratio) at 6 mL/min rate. The experiment was performed under a steady stream of nitrogen to avoid oxidation. The particle sizes were in the range of 5.6–16.8 nm. The peaks of the particles' absorption bands at 205 nm and 291 nm are attributed to the oscillations of the surface plasmons, and the calculated band gap of the particles is 1.97 eV. Based on the extract, 30-fold single-phase magnetite nanoparticles are formed with a reduced band gap compared to the raw Fe_3O_4 nanoparticles. The obtained NPs demonstate good water-disperse and hydrophilic properties.

Khatami et al. [139] synthesized superparamagnetic iron oxide nanoparticles (SPIONs) using a zero-calorie natural sweetener (Stevia) for reduction and stabilization. SPIONs (less than 25 nm) were very stable due to the biomolecular coating, as the zeta potential (-41.1 mV) creates opposite forces between the nanoparticles and prevents them from assembling. Biogenic SPIONs were able to counteract the effects of oxidative metabolites, according to a study of antioxidant activity. Figure 7c shows VSM magnetization curves of iron oxide nanoparticles. The FE-SEM image of the synthesized SPIONs is shown in Figure 7d. Great magnetic and catalytic properties, biocompatibility and low toxicity prove their potential for biomedical applications.

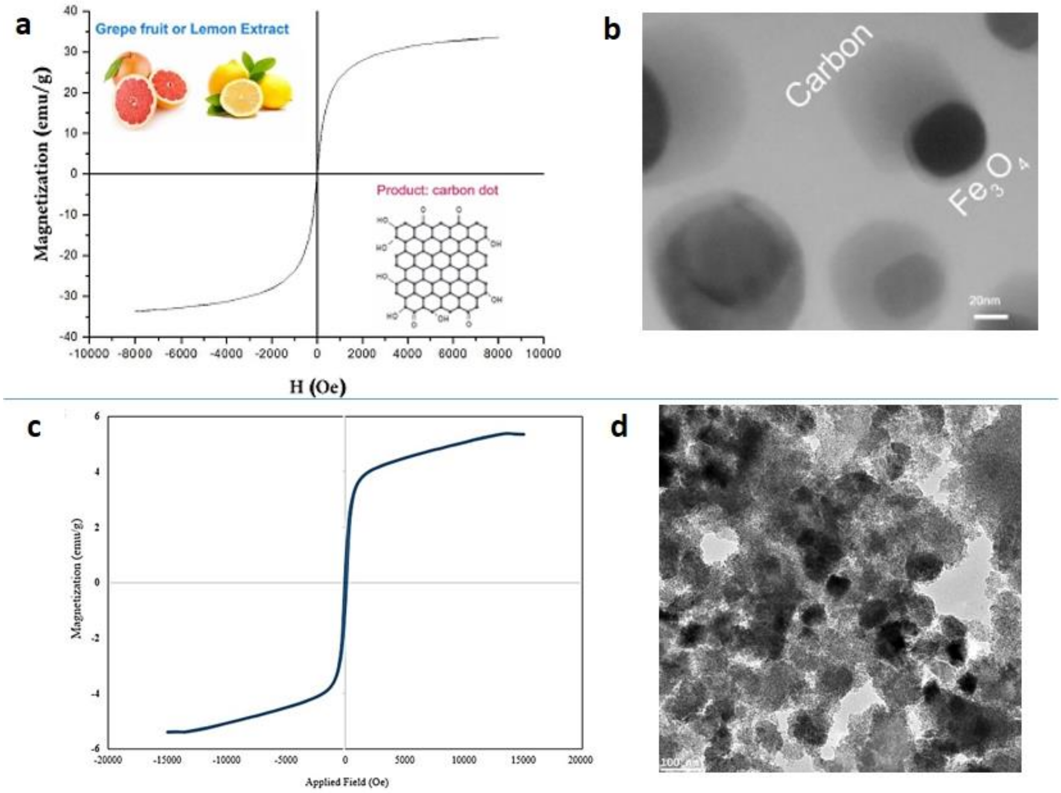

Figure 7. (**a**) VSM curve and (**b**) TEM image of Fe3O4-CDs nanocomposite obtained using lemon extract (Adapted with permission from [137], Elsevier, 2018); (**c**) The VSM magnetization curves and (**d**) FE-SEM image of iron oxide nanoparticles, synthesized using a zero-calorie natural sweetener (Stevia) (Adapted with permission from [139], Elsevier, 2019).

The food industry expresses great interest in β-glucosidase enzyme because of its role in the transformation of food to obtain functional foods. Moradi et al. [140] covalently immobilized β-glucosidase on aminotanic acid modified with magnetic Fe_3O_4 nanoparticles (ATA-Fe_3O_4 MNPs) as a biocompatible nanoplatform with a modified polyaldehyde pullulan to increase the ability and strength of the nanoparticle to bind the enzyme. The highest percentage of loading and immobilization yield was obtained with a solution of 0.1 mg of enzyme per 1 mL of citrate buffer (pH = 6; 1 M), a solution of citrate buffer carrier (ATA-Fe_3O_4)—10 mg/3 mL (pH = 6; 1 M) and a solution of polyaldehyde pullulan—20% of the total volume of the reaction system. Optimal pH and temperature values were found for free enzyme (pH = 5; 30 °C) and immobilized enzyme (pH = 6; 40 °C). The immobilized β-glucosidase enzyme retains its activity up to 83% after 10 cycles, so its immobilization by this method is an effective way for improving the properties of the enzyme. Magnetic hysteresis loops of the Fe_3O_4 MNPs, ATA-Fe_3O_4 MNPs, BGL-ATA-Fe_3O_4 MNPs are shown in Figure 8a. Figure 8b shows TEM image of the ATA-Fe_3O_4 MNPs.

Karade et al. [141] received magnetic Fe_3O_4 nanoparticles (with particle sizes from ∼20 to 25 nm) via modified "green" synthesis method using green tea extract as a reductant and ethylene glycol as a solvent. As observed, the reaction time strongly affected the magnetic and structural properties of magnetic nanoparticles. As time increased, the crystallite size also increased from 7.5 to 12 nm with an improvement in saturation magnetization (Figure 8c,d). Magnetic measurements revealed that nanoparticles were superparamagnetic at room temperature, ferromagnetic and superparamagnetic—at 60 K. Magnetite magnetic nanoparticles synthesized using green tea extract are promised for bioapplication due to their biocompatibility and high magnetization.

Fatimah et al. [142] used *Parkia speciosa* husk extract for the synthesis of magnetic nanoparticles. The obtained NPs consisted from magnetite and hematite particles with sizes in the range of 10–80 nm. The magnetic NPs exhibited an excellent photocatalytic properties in the degradation of the bromophenol blue dye under UV and visible light. The synthesized "green" nanoparticles are promising as photocatalysts in the degradation of dyes from wastewater.

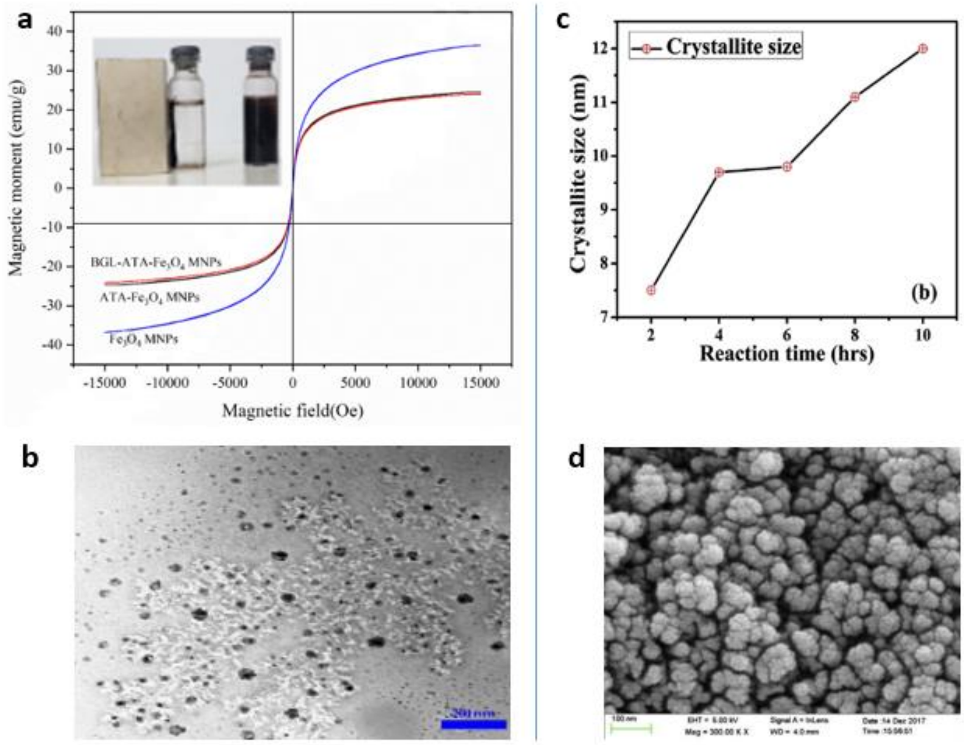

Figure 8. (**a**) Magnetic hysteresis loops of the Fe_3O_4 MNPs, ATA-Fe_3O_4 MNPs, BGL- ATA-Fe_3O_4 MNPs and (**b**) TEM image of the ATA-Fe_3O_4 MNPs (Adapted with permission from [140], Elsevier, 2019); (**c**) Change in crystallite size as a function of reaction time and (**d**) FE-SEM image of Fe_3O_4 MNPs synthesized using green tea extract (Adapted with permission from [141], Elsevier, 2018).

4.4. "Green" Synthesis of Spinel Magnetic Nanoparticles

Spinel ferrites with the general formula AB_2O_4 have great chemical, catalytic, adsorption and magnetic properties [143–148]. Spinel ferrites have attracted much attention due to their thermal and chemical resistance [149–154]. Nickel ferrite ($NiFe_2O_4$) is a major representative of spinel ferrites with the inverse spinel structure, which demonstrates ferromagnetism, originating from the magnetic moment of the antiparallel spins of metal ions (Ni^{2+} and Fe^{3+}) [155]. Udhaya et al. [156] developed a simple auto-combustion method using albumen for the synthesis of nanocrystalline nickel ferrite ($NiFe_2O_4$). Egg white (albumen), which is used in the "green" synthesis, plays the role of fuel in the process of auto-combustion. The results of powder analysis and IR spectroscopy indicated that the synthesized nanoparticles are single-phase and the spinel structure is cubic with a particle size of 23 to 47 nm. The dielectric properties of the nickel ferrite were measured for different frequencies from 100 Hz to 1 MHz. It was concluded that the alternating conductivity increases with increasing frequency.

Al-Hunaiti et al. [157] developed a "green" synthesis of magnetic $CuFe_2O_4$ NPs with an average size of 20 nm using *Azadirachta indica* extract. Cupper ferrite NPs were tested as an effective catalyst for the arylalkanes oxidation without solvents, especially in direct oxidation of toluene to obtain the desired benzoic acid in mild and eco-friendly conditions.

Routray et al. [158] synthesized nanosized $CoFe_2O_4$ via automatic combustion method using *Aloe vera* and the solutions of precursors $Fe(NO_3)_3{\cdot}9H_2O$ and $Co(NO_3)_2{\cdot}6H_2O$. FE-SEM microphotographs revealed the formation of a bud-like structure and the resulting particle size was approximately 50–65 nm. Magnetic properties, especially saturation magnetization, remanence magnetization and coercivity, were examined from the M-H loops: 72.23 emu/g, 31.29 emu/g, 1519 Oe, respectively. Furthermore, a massive dielectric constant, low dielectric loss and variable conductivity of $CoFe_2O_4$ nanoparticles depended on the frequency (100 Hz–1 MHz), preparation method and grain size.

Madhukara Naik et al. [151] prepared spinel zinc ferrite ($ZnFe_2O_4$) nanoparticles using the juice of *Limonia acidissima* (wood-apple). $ZnFe_2O_4$ nanoparticles were obtained by adding zinc nitrate and ferric nitrate to 5 mL of *Limonia acidissima* juice (reducing agent). The proposed method leds to obtain $ZnFe_2O_4$ nanoparticles with an average crystallite size of 20 nm (Figure 9a). The study of magnetic properties reveals a high saturation magnetization of $ZnFe_2O_4$. $ZnFe_2O_4$ nanoparticles exhibited effective photodegradation of Evans blue and methylene blue dyes when exposed to visible light. Furthermore, the antibacterial activity (Figure 9b) of the nanoparticles was investigated against both gram-negative and gram-positive bacteria.

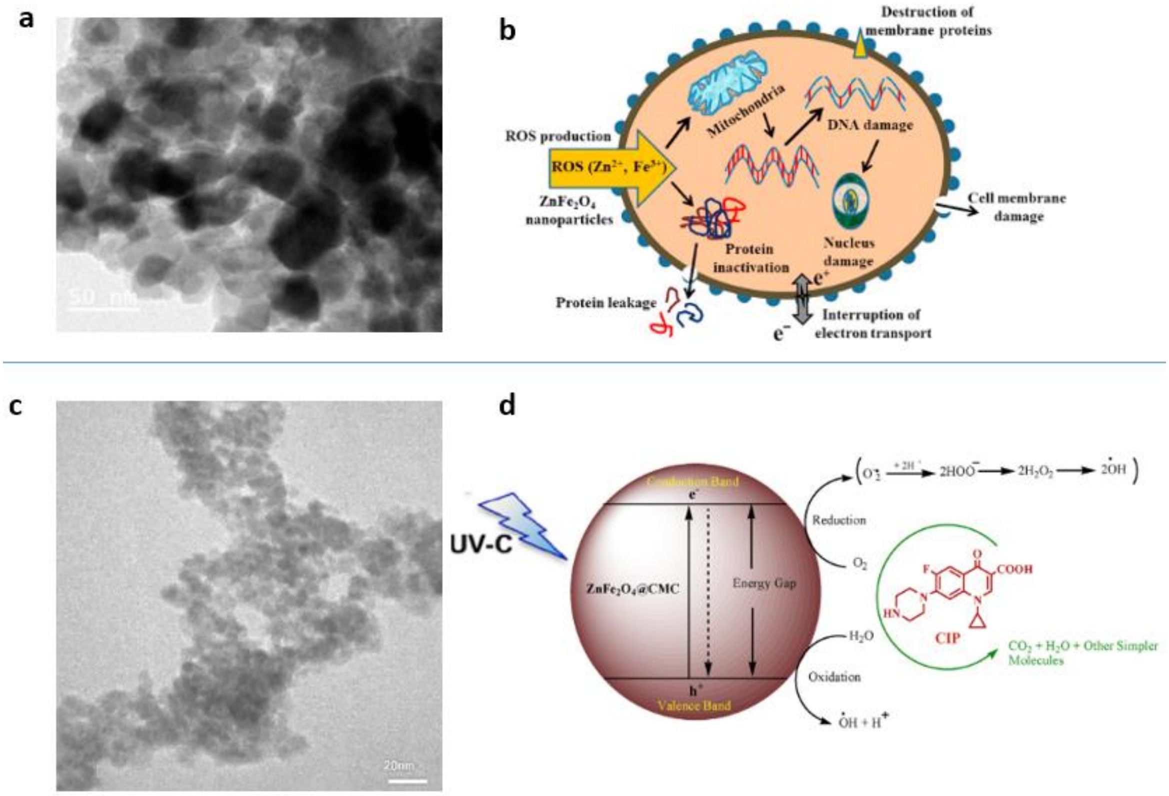

Figure 9. (**a**) TEM image and (**b**) antibacterial activity mechanism of microwave-assisted green synthesis of $ZnFe_2O_4$ nanoparticles (Adapted with permission from [151], Elsevier, 2019); (**c**) TEM image of $ZnFe_2O_4$@CMC as a prepared photocatalyst for degradation of CIP and (**d**) mechanism for photodegradation of CIP by nano $ZnFe_2O_4$@CMC (Adapted with permission from [159], Elsevier, 2019).

Ciprofloxacin (CIP) is an antibiotic that is widely used to treat infections. It is mostly excreted in non-metabolized form and enters the water via wastewater discharge. The aim of research by Malakootian et al. [159] was to synthesize $ZnFe_2O_4$@CMC and investigate its effectiveness in removing CIP during the photocatalytic process. The authors successfully synthesized the nanobiocomposite $ZnFe_2O_4$@CMC via hydrothermal method. Initially, $Fe(NO_3)_3{\cdot}9H_2O$ та $Zn(NO_3)_2{\cdot}6H_2O$ were dissolved in a 2:1 ratio in 100 mL of deionized water. Then 0.5 g of carboxymethylcelluloce (CMC) and 6 g of NaOH was being gradually added over an hour to obtain a suspension with pH = 12. After 30 min, a suspension of dark brown color was obtained and placed in the oven at 160 °C for 20 h. The acquired precipitate was washed and dried at 60 °C for 2 h. TEM image of $ZnFe_2O_4$@CMC as a prepared photocatalyst for degradation of CIP is shown in Figure 9c. The photocatalytic activity of $ZnFe_2O_4$@CMC was evaluated by studying the effect of reaction time (20–120 min), the initial concentration of CIP (5–30 mg/L), pH (3–11), the dose of photocatalyst (0.1–0.5 g). The optimal conditions for maximum removal efficiency in synthetic (87%) and natural (79%) samples were: pH = 7, initial CIP concentration—5 mg/L, photocatalyst dose—0.3 g and irradiation time—100 min. Kinetic studies have shown that photocatalytic degradation of CIP is accompanied by pseudo-first-order kinetics. Mechanism for photodegradation of CIP by nano $ZnFe_2O_4$@CMC is shown in Figure 9d. The new magnetic nanobiocomposite $ZnFe_2O_4$@CMC has demonstrated good chemical stability and reusability after five cycles.

Saeid Taghavi Fardood et al. [160] reported non-toxic, cheap, and eco-friendly route using tragacanth gel to synthesize superparamagnetic nanoparticles of magnesium ferrite ($MgFe_2O_4$). The $MgFe_2O_4$ NPs exhibits excellent photocatalytic properties for Malachite green dye removal (98%) when exposed to visible light. The $MgFe_2O_4$ catalyst demonstrate good reusability during six cycles and can be easily removed from solution by magnetic separation.

Gayathri Manju et al. [161] prepared nickel-copper ferrite nanoparticles [$Cu_{1-x}Ni_xFe_2O_4$ (x = 0, 0.5, 1)] via combustion method using *Aloe barbadensis* extract as a "green" reducing agent. XRD patterns confirmed the formation of compositions with a cubic spinel structure and a crystallite size of 52 nm shrinked to 29 nm after adding nickel to copper ferrite and to 35.85 nm for nickel ferrite. Measurements of magnetization received at room temperature indicated mild ferromagnetic behavior and saturation magnetization, and the coercivity value increased with nickel substitution. A study of antibacterial activity against *Bacillus subtilis*, *S. aureus*, *Klebsilla pneumonia* and *E.coli* was performed using diffusion method. The results showed increased activity when adding nickel to copper ferrite.

Atrak et al. [162] synthesized $Mg_{0.5}Ni_{0.5}Al_xFe_{2-x}O_4$ (x = 0.5, 1, 1.5) spinel ferrites by a "green" sol-gel method using tragacanth gel (Figure 10a,b). It was shown that the crystallite size decreased with increasing concentration of Al^{3+}. Studies of the optical bands energy gap in the samples show that the value of the band gap increases from 2.55 to 2.67 eV due to increase in the dosage of Al^{3+}. Photocatalytic activity was evaluated during the degradation of the direct blue 129 (DB129) dye as a model reaction of environmental pollution when exposed to visible light. Experimental results confirmed a direct relation between photocatalytic activity and the amount of Al: a catalyst with x = 1.5 illustrates better degradation (94%) than a catalyst with x = 1 (88%) and x = 0.5 (79%).

Mahajan et al. [153] synthesized $CoFe_4O_4$ NPs and $Ag_xCo_{1-x}Fe_2O_4$ NPs (where x = 0, 0.005, 0.01, 0.02) via sol-gel autocombustion method using "green" and chemical synthesis with extracts from tulsa seed (*Ocimum sanctum*) and garlic cloves (*Allium sativum*). The XRD analysis confirmed that the prepared samples were crystalline and had a cubic spinel (inverse) structure. Magnetic measurements at room temperature showed that the saturation magnetization values for samples obtained using tulsa seed extract (49.72 emu/g) and chemical synthesis (49.95 emu/g) were significantly higher than those obtained using garlic extract (28.89 emu/g) (Figure 10c). FE-SEM micrograph of Ag 1% doped chemically synthesized $CoFe_2O_4$ nanoparticles is shown in Figure 10d. The samples demonstrated good antibacterial activity: they were more effective against gram-positive than against gram-negative bacteria, mainly due to the difference in the bacterial cell wall.

Madhukara Naik et al. [152] prepared nanostructured Zn-doped cobalt ferrites $Zn_xCo_{1-x}Fe_2O_4$ (x = 0.0 to 0.6) via combustion method using cheese as "green" fuel. X-ray diffraction patterns reveal that these nanomaterials have a crystallite size in the range of ~12–21 nm with an inverse cubic spinel structure. Figure 11a shows CIE diagram of $Zn_xCo_{1-x}Fe_2O_4$ NPs. The vibrational stretching modes of the tetrahedral (582 cm^{-1}) and octahedral (385 cm^{-1}) sections (metal-oxygen bonds) were confirmed by IR spectra. Photodegradation studies of the obtained nanoparticles were examined during degradation of Congo red and Evans blue dyes under visible light (Figure 11b). Pure $CoFe_2O_4$ nanoparticles and Zn-doped $CoFe_2O_4$ NPs were examined against both gram-positive (*S. aureus*) and gram-negative (*S. typhi*) bacteria. Gram-negative bacteria *Salmonella typhi* exhibit high antibacterial activity in a zone of inhibition of Zn-doped $CoFe_2O_4$ (22 mm), compared with pure $CoFe_2O_4$ (16 mm). The obtained nanoparticles are suitable for optoelectronic, photocatalytic and pharmaceutical applications.

Moradnia et al. [154] obtained $MgFeCrO_4$ magnetic nanoparticles of spinel structure via a "green" sol-gel synthesis method. Tragacanth gel was used to provide a comfortable, natural and cheap sol-gel method that does not contain surfactants and organic solvents. X-ray diffraction patterns confirmed the formation of spinel cubic magnetic $MgFeCrO_4$ nanoparticles. Figure 11c shows magnetic hysteresis loop of spinel $MgFeCrO_4$ nanoparticles, and Figure 11d shows TEM image pattern of $MgFeCrO_4$ MNPs. The unique photocatalytic activity of magnetic $MgFeCrO_4$ nanoparticles for rapid degradation of direct black 122 (DB122) dye in aqueous solution under visible light was studied. The photocatalytic activity of the nanocatalyst ($MgFeCrO_4$) is achieved due to the synergistic effect between Mg, Fe and Cr in the spinel structure. This nanocatalyst is heterogeneous (insoluble in water) and stable during photodegradation. The results showed that 96% of the DB122 dye was degraded in only 60 s. The degradation kinetics of DB122 are consistent with the pseudo-first-order kinetic model. Magnetic $MgFeCrO_4$ nanoparticles show excellent reusability for DB122 dye degradation, as the photocatalyst did not show a significant reduction in its activity even after four applications. The synthesized magnetic nanoparticles have a promising potential for use in electrical and optical systems, cosmetology, ecology, etc.

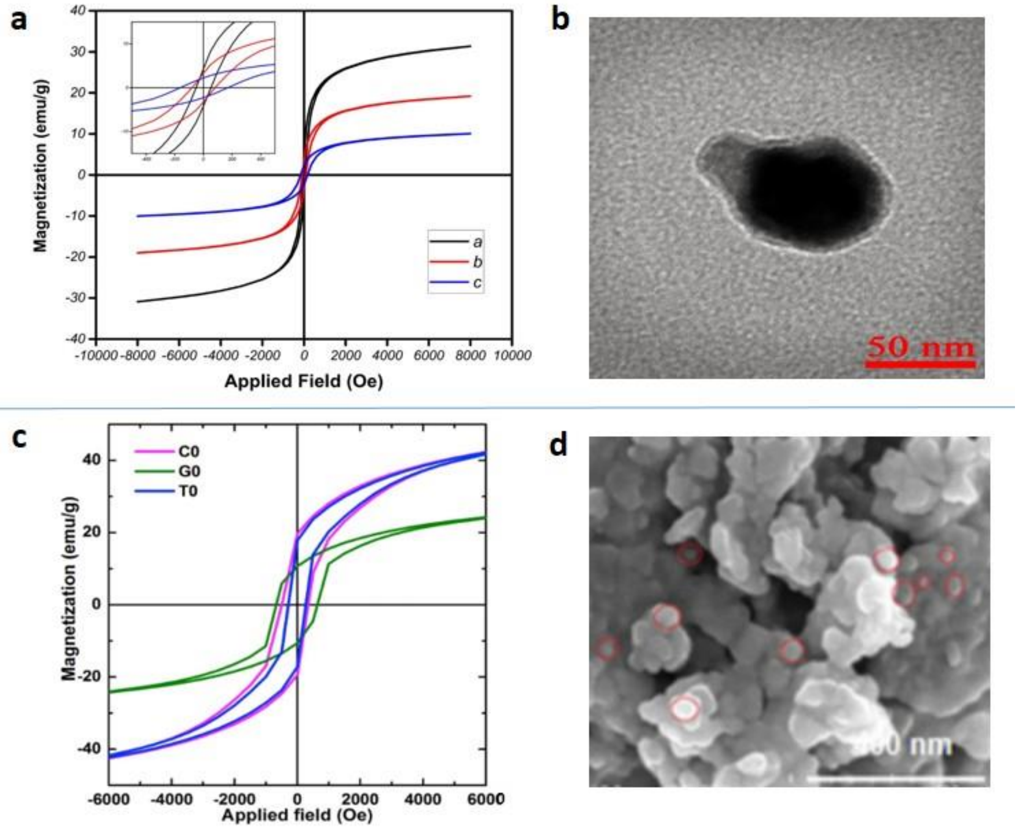

Figure 10. (**a**) Magnetic hysteresis loops of spinel $Mg_{0.5}Ni_{0.5}Al_xFe_{2-x}O_4$ (a: x = 0.5; b: x = 1; c: x = 1.5) obtained using tragacanth gel (Adapted with permission from [162], Elsevier, 2019); (**b**) TEM images of $Mg_{0.5}Ni_{0.5}Al_xFe_{2-x}O_4$ MNPs (x = 0.5) (Adapted with permission from [162], Elsevier, 2019); (**c**) magnetic properties and (**d**) FE-SEM micrograph of Ag 1% doped $CoFe_2O_4$ nanoparticles, synthesized using green extract of garlic and tulsi seed (Adapted with permission from [153], Elsevier, 2019).

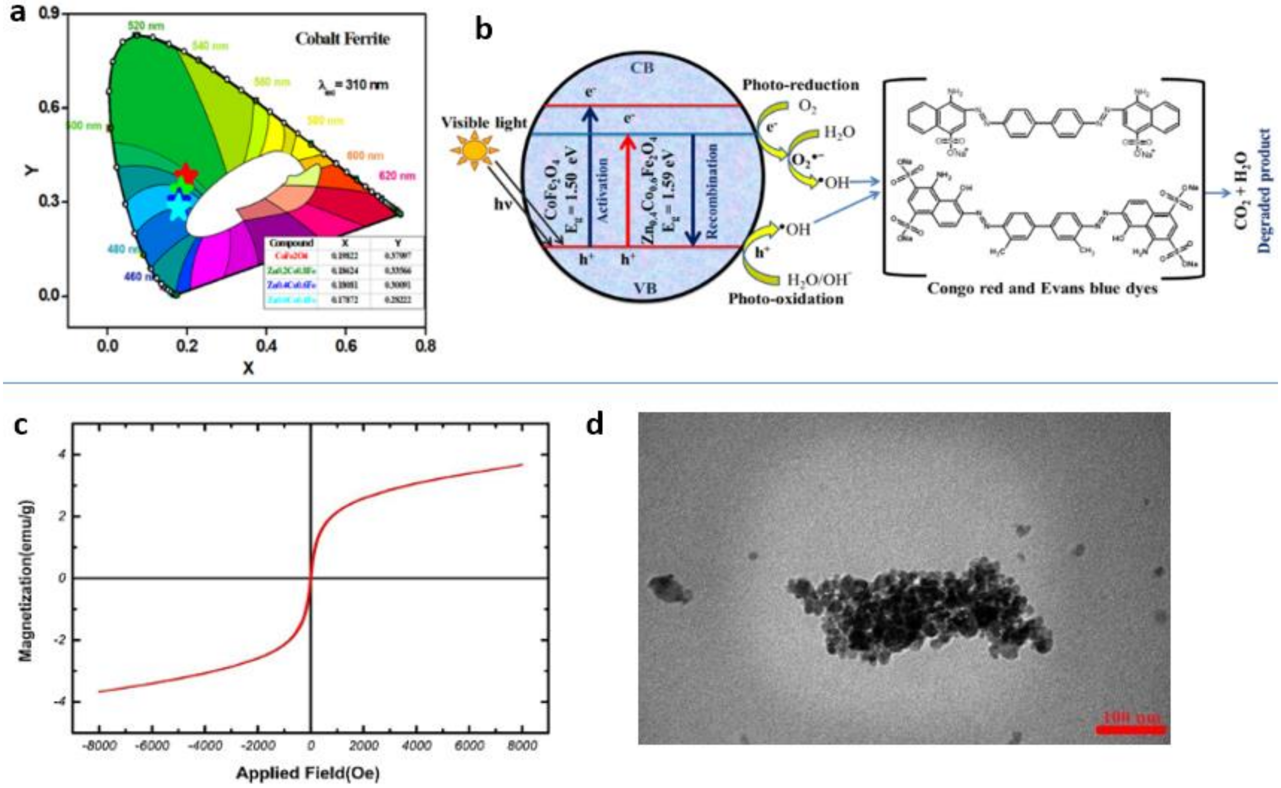

Figure 11. (**a**) CIE diagram of ZCF NPs and (**b**) possible reaction mechanism for the photocatalytic degradation of CR and EB dyes over ZCF NPs (Adapted with permission from [152], Elsevier, 2019); (**c**) Magnetic hysteresis loop and (**d**) TEM image of $MgFeCrO_4$ MNPs (Adapted with permission from [154], Elsevier, 2020).

5. "Green" Synthesis of Metal Nanoparticles

5.1. Silver Nanoparticles

Out of all noble metal nanoparticles, silver nanoparticles (AgNPs) are widely use in various fields, such as optic materials [163], photocatalysts [164–169], biomedicine [170–176], etc. For example, the general use of AgNPs in biomedicine can be attributed to their potent antibacterial properties against a wide range of bacteria. Various methods are used effectively to produce large numbers of AgNPs. However, these methods remain relatively expensive and usually require the involvement of certain harmful substances. Therefore, the development of "green" methods for obtaining silver nanoparticles is very important [177]. Recently, the obtaining of silver NPs using biological processes has attracted much attention. The use of plants and plant extracts is one of the most desirable methods of "green" biological synthesis due to their rich biologically active metabolites [178–186].

Aygün et al. [187] synthesized silver nanoparticles (AgNPs) using reishi mushroom extract (*Ganoderma lucidum*). 20 mL of mushroom extract was diluted to 100 mL by adding distilled water. Later, 15 mg of $AgNO_3$ salt was added to the mixture, which was then stirred magnetically until Ag^+ ions reduced to Ag^0 ions (transition from clear to brown-red color of the solution). In the UV-visible spectrum, a wide absorption peak between 400–460 nm was detected, indicating the presence of AgNPs. TEM images proved the nanoparticles had spherical shape with a diameter of 15–22 nm (Figure 12a). Antioxidant, antifungal and antimicrobial (against *S.aureus*, *E.coli*, *P.aeruginosa*, *L.Pneumophila*, *C. albicans strains*) activity of AgNPs were studied.

De Aragão et al. [188] offered a simple method of "green" route of AgNPs synthesis, using a polysaccharide extracted from red algae *Gracilaria birdiae*. AgNPs ranged between 20.2 nm and 94.9 nm (Figure 12b). AgNPs were examined for antimicrobial activity against *Escherichia coli* and *Staphylococcus aureus.* The obtained results prove that the silver nanoparticles, synthesized along with the polysaccharide, can be used for drug delivery.

Khatami et al. [189] synthesized AgNPs using dried grass. The average size of AgNPs was 15 nm (Figure 12c). It was investigated that such NPs demonstrate the antitumor, antibacterial and antifungal activity. When the concentration of AgNPs increases to five µg/mL, an inhibitory effect on the cancer cells growth is achieved, the survival of cancer cells is reduced by approximately 30%.

Saha et al. [190] presented a "green" eco-friendly method of AgNPs biogenic synthesis using *Gmelina arborea* fruit extract. The mixture of fruit extract and $AgNO_3$ was being heated at 60 °C along with continuous magnetical stirring at 1000 rpm. Within 5 min, the color of the solution changed from clear to yellowish. The formation of AgNPs was investigated via UV-visible spectra over the same period. A blank probe was prepared by taking 30 mL of distilled water instead of silver nitrate. The amount of added fruit extract ranged from 0.1 to 1.0 mL. TEM analysis proved that the AgNPs are stable, with spherical shape, and particle sizes ranging from 8 to 32 nm. The AgNPs hane been tested as "green" catalyst in Methylene blue dye degradation and demonstrated excellent catalytic properties.

M.R. Bindhu et al. [182] TEM image of AgNPs synthesized using *Moringa oleifera* flowers (Figure 12d). Transmission electron microscopy analysis indicated the formation of nanoparticles with spherical shape and size of 8 nm. Synthesized "green" AgNPs suppressed the growth of Klebsiella pneumonia and Staphylococcus aureus and effectively sensed Cu^{4+} ions.

Nouri et al. [191] synthesized ultra-small AgNPs using *Mentha aquatica* leaf extract. Phytochemicals from the extract can reduce Ag^+ to Ag^0 and form nanoparticles. The synthesis of AgNPs was carried out from $AgNO_3$ solution and at different pH (9, 9.5, 10 and 10.5), volume ratio of $AgNO_3$ solution to the extract (0.1: 0.9, 0.3: 0, 7, 0.5: 0.5, 0.7: 0.3, 0.9: 0.1 mL/mL), temperature (25, 40, 70, 90 °C) and ultrasound power (50, 100, 150 and 200 W). 0.5 mL of leaf extract was added to 19 mL of water, the pH was adjusted by adding 0.2M K_2CO_3 solution. Next, 0.5 mL of aqueous $AgNO_3$ solution (100 mM) was added dropwise, while continuously stirring magnetically or subjecting to ultrasound with a high-power ultrasonic generator tool equipped with a titanium tip. The formation of AgNPs through the reduction of Ag^+ to Ag^0 was monitored over different amounts of time via UV-spectroscopic analysis. To prevent unnecessary photochemical reactions, the vessel was covered with aluminum foil. Furthermore, all glassware was washed with a mixture of solutions of HCl and HNO_3 ($HCl{:}HNO_3 = 3{:}1$ v/v), and dried at 100 °C. The obtained AgNPs were washed and centrifuged at 16,000 rpm. The effective synthesis parameters were fully optimized to achieve small size of nanoparticles (8 nm) (Figure 12e) with superior antibacterial properties. In particular, the values of the minimum inhibitory concentration for ultrasonically synthesized AgNPs against *P. aeruginosa*, *E. coli*, *B. cereus* and *S. aureus* were 2.2, 58, 20 and 198 µg/mL, respectively. In addition, those AgNPs have shown significant catalytic activity for the removal of various types of dyes, which are environmental contaminants.

Ravichandran et al. [167] performed a "green" synthesis of AgNPs via bioreduction of silver nitrate using an *Parkia speciosa* leaf extract. The change of the solution color to brown indicated the biological reduction of $AgNO_3$: 1 mL of 0.01M $AgNO_3$ solution was added to 1 mL of *Parkia speciosa* leaf extract in a 10 mL volumetric flask, which was filled to 10 mL with deionized water and kept at room temperature for 24 h. The synthesized AgNPs were centrifugated at 10,000 rpm. The synthesized AgNPs demonstrated maximum absorption at 410.5 nm. SEM and TEM (Figure 12f) analyses revealed the average size of AgNPs (31 nm and 35 nm, respectively). The synthesized AgNPs demonstrate good photocatalytic (in Methylene blue dye degradation), antimicrobial (against *Bacillus subtilis, Pseudomonas aeruginosa, Staphylococcus aureus* and *Escherichia coli*) and antioxidant activity. Synthesized AgNPs can be used in various fields, such as water purification, biomedicine, biosensors and nanotechnology.

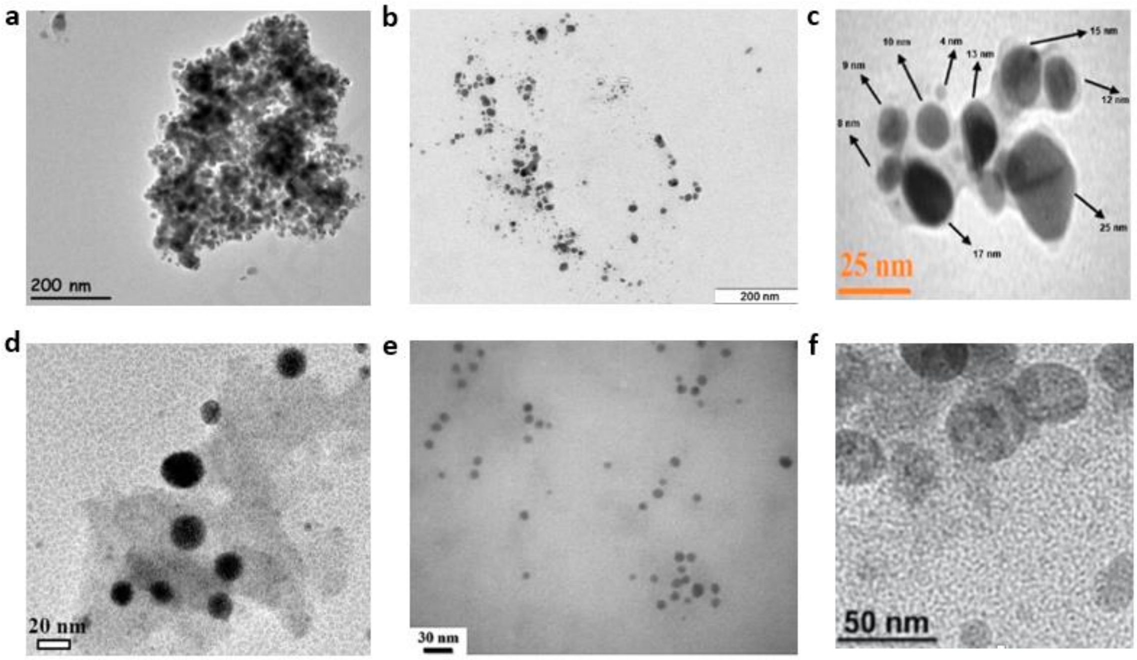

Figure 12. (**a**) TEM image of AgNPs (Adapted with permission from [187], Elsevier, 2020); (**b**) TEM image for AgNPs obtained at pH 11 (Adapted with permission from [188], Elsevier, 2019); (**c**) TEM image of biosynthesized silver nanoparticles (Adapted with permission from [189], Taylor & Francis, 2018); (**d**) TEM image of AgNPs synthesized using *Moringa oleifera* flowers (Adapted with permission from [182], Elsevier, 2020); (**e**) TEM image of AgNPs synthesized by sonochemical method (Adapted with permission from [191], Elsevier, 2020); (**f**) TEM image of AgNPs, obtained using Parkia speciosa leaves extract (Adapted with permission from [167], Elsevier, 2019).

Odeniyi et al. [192] investigated the phytochemical, antioxidant and antimicrobial potential of aqueous and methanolic extracts of *Nauclea latifolia* fruit and their application in the biosynthesis of AgNPs and for cold cream formulations. The extracts were used to bioreduce silver nitrate to AgNPs. Phytochemical evaluation of crude *Nauclea latifolia* extracts showed the presence of alkaloids, terpenoids, flavonoids, saponins, anthraquinones, steroids, and tannins. The plasmon resonance peak was at 350 nm, and such functional groups as hydroxyl, carboxyl, alkyl halide, phenolic, amine, carbonyl, and amide were important for bioreducing and closing silver ions into nanoparticles. The analysis showed that silver is the main element, and nanoparticles have an irregular shape and size of 12 nm. The obtained creams were stable, cosmetically attractive with satisfactory pH, viscosity and application. Silver nanoparticles based on aqueous extracts of *Nauclea latifolia* and its cream composition showed strong antimicrobial and antioxidant activity.

5.2. Gold Nanoparticles

Gold nanoparticles (AuNPs) are considered the most attractive among noble metal nanoparticles, because of their potential use in catalysis, optics, biomedicine, etc. The widespread application of AuNPs has aroused considerable interest for new AuNPs synthesis methods, avoiding hazardous chemicals [53,177,193–196]. Alternative methods, including "green" synthetic approaches to produce AuNPs, are important for maintaining sustanable development.

Molnár et al. [197] showed and compared results of few approaches to the synthesis of AuNPs using fungal strain. Izadiyan et al. [194] used an improved method of two-stage synthesis to form "core-shell" type Fe_3O_4/Au nanostructures from the extract of *Juglans regia* green husk. The Fe_3O_4 NPs were suspended in $HAuCl_4$ solution, and the molar ratio in solution was adjusted to 1:1. Iron oxide nanoparticles suspended in $HAuCl_4$ solution were subjected to ultrasound for 20 min. *J. regia* extract was added as a reductant and stabilizer. Next, Fe_3O_4/Au was autoclaved at 120 °C for 20 min, the supernatant was discarded and oven dried at 60 °C. The Fe_3O_4/Au NPs demonstrate magnetic properties (Figure 13a) and average diameter is around six nm (Figure 13b). The anticancer activity of Fe_3O_4/Au NPs may be promised candidates for cancer treatment and other biomedical applications.

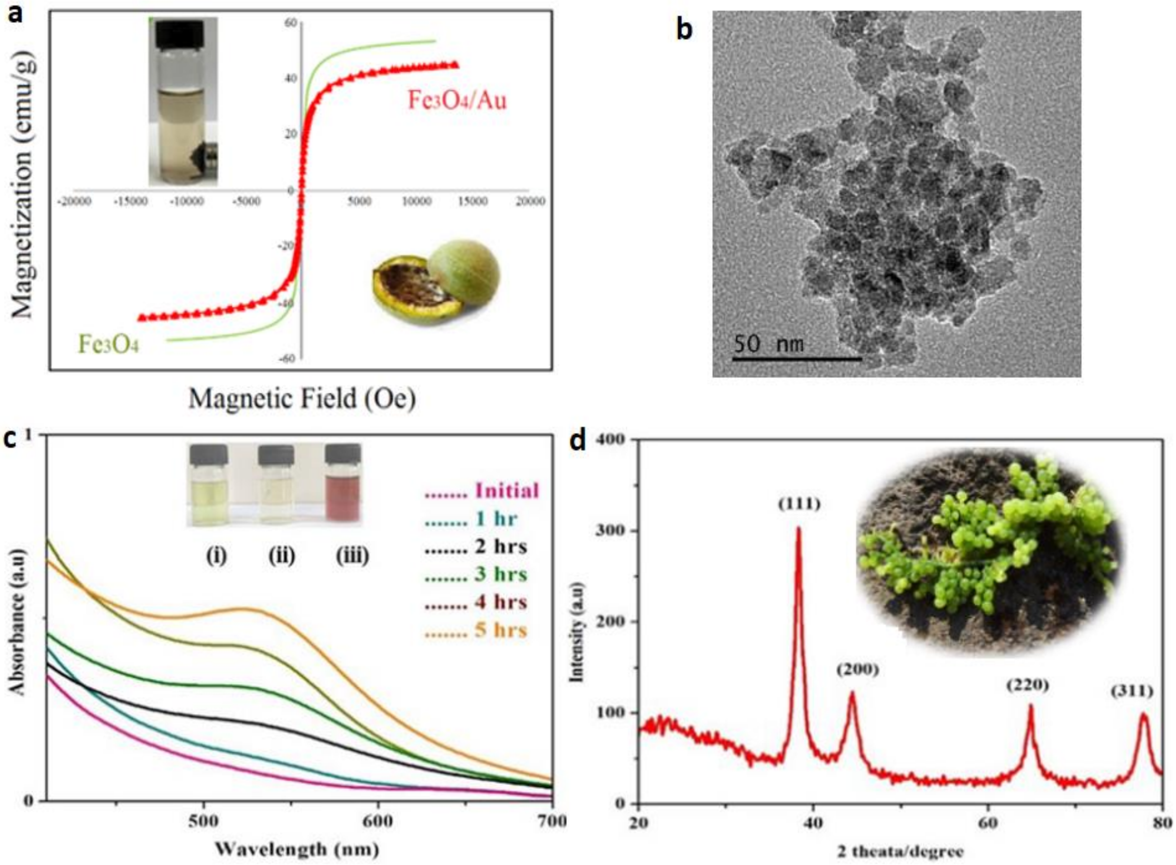

Figure 13. (**a**) Vibrating sample magnetometer plots of Fe_3O_4 and Fe_3O_4 coated with Au nanoparticles (Adapted with permission from [194], Elsevier, 2019); (**b**) HR-TEM image of Fe_3O_4/Au nanoparticles (Adapted with permission from [194], Elsevier, 2019); (**c**) UV-Visible spectrum of Cr@AuNPs. The inserted figure shows the color changes of Cr@AuNPs, (i) extract, (ii) chloroauric acid and, (iii) synthesized Cr@AuNPs (Adapted with permission from [198], Elsevier, 2019); (**d**) XRD pattern of Cr@AuNPs (Adapted with permission from [198], Elsevier, 2019).

Manikandakrishnan et al. [198] reported using *Caulerpa racemosa* (Cr) to synthesize gold nanoparticles (AuNPs). *C. racemosa* extract mixed with $HAuCl_4$ solution under stirring (24 h) and the Cr@AuNPs were obtained (Figure 13c). The presence of phytochemical components in the aqueous extract of *C. racemosa* was confirmed by IR spectroscopic analysis. The size of Cr@AuNPs ranged from 13.7 to 85.4 nm. XRD pattern of Cr@AuNPs is shown in Figure 13d. The synthesized Cr@AuNPs effectively controlled the growth of human colon adenocarcinoma cells (HT-29), and demonstrated IC_{50} of 20.84 µg/mL. "Green" synthesized Cr@AuNPs had a non-toxic effect on *Artemia nauplii*, even at high concentrations (100 µg/mL).

Shabestarian et al. [199] developed a "green", eco-friendly, fast and simple synthesis of AuNPs using aqueous *Sumac* extract. The solution of $HAuCl_4$ mixed with aqueous *Sumac* extract and the purple solid was obtained. The TEM analysis revealed that the bio-formed AuNPs have a spherical morphology with an average size of 20 nm. The antioxidant activity of the bio-formed AuNPs has been tested. It was concluded that such AuNPs are promising for biomedical applications.

5.3. Platinum Nanoparticles

Platinum nanoparticles (PtNPs) have been widely used in oxidation and hydrogenation reactions in petrochemical industry, due to their large surface and many other characteristics that encourage to synthesize PtNPs for catalytical applications. Therefore, there is a high demand for synthesis of PtNPs using of eco-friendly materials [177,200–205].

Kumar et al. [201] used *Xanthium strumarium* leaf extract for the biosynthesis of PtNPs. TEM analysis confirmed the formation of PtNPs with an average size of 22 nm, and SEM analysis revealed that those PtNPs have a cubic and rectangular shape and smooth surface. The nanoparticles demonstrated huge cytotoxic effect on HeLa cell lines, thus can be used for biomedical applications.

Dobrucka [203] presented „green" synthesis of PtNPs using *Fumariae herba* extract. TEM analysis showed hexagonal and pentagonal shapes of synthesized PtNPs with a diameter of 30 nm. PtNPs demonstrated high catalytic activity during reduction of violet crystal and methyl blue dyes.

Al-Radadi et al. [200] performed a "green" synthesis of PtNPs using an extract solution of dates (biodegradable surfactants) in order to learn about their effect on various cancer cells. Aqueous extracts of solutions from Ajwa and Barni dates behave as stabilizers and reductants in the synthesis of PtNPs in natural environment conditions. The size of obtained PtNPs was small, in the range of 1.3-2.6 nm. Furthermore, the change of pH in the reaction affected the size of nanoparticles. Antitumor activity of PtNPs was tested for various cancer cells: carcinoma cells (HCT-116), breast cancer cells (MCF-7) and hepatocellular carcinoma (HePG-2). Antibacterial activity of PtNPs against *Escherichia coli* and *Bacillus subtilis* bacteria was study and were found that PtNPs are able to inhibit the growth of *E. coli* and *B. subtilis*.

5.4. Palladium Nanoparticles

Palladium nanoparticles (PdNPs) are being used in various unique applications, including sensors and active membrane catalysts, thanks to their catalytic properties and hydrogen affinity. PdNPs are synthesized using a variety of wet chemical approach, such as chemical reduction, electrochemical and polyol methods [177].

„Green" synthesis of PdNPs for catalysis and biological applying is of enormous interest [206–213]. Lentinan (LNT) can be a fine stabilizing and reducing agent for replacing complex plant extracts. Han et al. [214] showed a simple "green" method of PdNPs synthesis using LNT as a stabilizer to achieve a smaller Pd_n-LNT nanoparticles (2.35–3.32 nm), as well as a higher catalytic activity for the 4-nitrophenol reduction, comparing to other known catalysts. Furthermore, Pd_n-LNT NPs demonstrated insignificant cell cytotoxicity along with good antioxidant activity.

Celebioglu et al. [215] synthesized PdNPs loaded on cyclodextrin (CD) nanofibers. Cyclodextrin acted as a reductant and catalyzed the PdNPs formation upon reduction from Pd^{2+} to metallic Pd^0. The results of the study confirmed the presence of homogeneously distributed polycrystalline PdNPs (3–5 nm) in the entire nanofiber matrix and shown the existing of a larger fraction of the metal Pd^0 atom due to effective reduction of Pd^{2+} by CD molecules. Catalytic properties of PdNPs were evaluated through reduction of n-nitrophenol to n-aminophenol, resulting in high catalytic activity of nanofibers.

Amrutham et al. [216] synthesized nano-sized PdNPs via a new, single-stage and cheap method with high yield—microwave irradiation using water-soluble Neem wood resin as a stabilizer and reductant. The resin was purified and washed thoroughly with double distilled water. An aliquot of 50 mL of an aqueous H_2PdCl_4 solution (5×10^{-4} M) was added to 50 mL of a 1% resin aqueous solution. The reaction took place in a microwave oven at 320 W for 10 min. The average particle size was about four nm. Catalytic activity of PdNPs was evaluated spectrophotometrically through reduction of Rhodamine 6 G dye using $NaBH_4$. PdNPs, stabilized with Neem wood resin, demonstrated excellent catalytic activity for Rhodamine 6 G reduction (18 min). The reaction showed pseudo-first order kinetics, and the obtained rate constant equaled 0.1875 min^{-1}.

6. Future Perspectives

Thus, green chemistry is an ecological branch of chemistry that aims to minimize the use of toxic and hazardous chemicals. There are several main ways to maximize the implementation of the principles of "green" chemistry in all spheres of life:

(1) to create various chemical associations, organizations and institutes, whose missions will be studying of cleaner reactions, products and processes;
(2) to promote "green" chemistry among universities and research laboratories in order to develop economically sustainable technologies for clean production;
(3) to introduce methods of "green" synthesis of chemicals in industrial enterprises;
(4) to train future scientists in universities, who in the future will solve regional and global environmental problems (nowadays, most industrial developments are related mainly to economic efficiency, rather than environmental friendliness of processes);
(5) to ensure environmental protection at the legislative level;
(6) to use innovative alternative methods of minimal production of undesired chemicals in order to preserve human health and reduce harmful effects on the environment, namely: use alternative (renewable) sources of raw materials; use less hazardous reagents; use alternative solvents (ionic liquids, water, etc.) during the synthesis of organic matter; use "green" catalysts that affect energy consumption and reduce the production of unwanted by-products and waste; minimize energy consumption at every stage of the industrial process.

In future, "green" chemistry should be applied to almost every sector of the business—food industry, energy, plastics, medicines, cosmetics, cleaning products, etc., and therefore it will play an important role in the industry development.

7. Conclusions

This review reveals basic principles of "green" chemistry and "green" methods for obtaining metal/metal oxide nanoparticles using bioresources. The most common method for obtaining these nanoparticles is a "bottom-up" approach, using various organic solvents, toxic chemicals and non-ecological reagents under high pressure and temperature. Therefore, alternative, cheap and safe methods are necessary. "Green" synthesis prevents pollution during initial stages of chemical processes and reduces the negative impact on the environment and human health. Many interesting biological methods using plants, algae, fungi, yeast, bacteria, viruses, etc., have been developed. Among various "green" resources, plants are the best source of precursors for the synthesis of metal/metal oxide nanoparticles, due to their simplicity, non-toxicity and availability. Such parameters as total antioxidant capacity and total protein content affect the suitability of plants. It is important to study physical and chemical properties, stability and activity of "green" nanoparticles in order to further improve their practical application. This review involves using sol-gel method, hyperthermal method, auto-combustion, etc., for the synthesis of magnetic nanoparticles. Various extracts of plants, including leaves of *Lagenaria siceraria*, *Aloe vera*, *Averrhoa carambola*, husk of *Punica Granatum*, roots of *Mimosa pudica*, *Chromolaena odorata*, etc., are frequently used as reductants. The separate section is dedicated to „green" synthesis and the use of spinel magnetic nanoparticles (in particular, superparamagnetic Fe_3O_4 NPs), which attracted the attention of researchers due to their unique properties: bio-degradability, biocompatiblity and non-toxic effect. The biocompatibility and high saturation magnetization of naturally stabilized magnetic nanoparticles allows for their various biological applications. Methods of "green" synthesis of silver, gold, platinum and palladium nanoparticles are also described. For reduction and stabilization during the synthesis of AgNPs, extracts of reishi mushroom (*Ganoderma lucidum*), red algae (*Gracilaria birdiae)*, *Gmelina arborea* fruit, *Nauclea latifolia* fruit, *Mentha aquatica* leaves and *Parkia speciosa* leaves have been used. For the synthesis of AuNPs, *Juglans regia* green husk extract, *Caulerpa racemose* extract and *Sumac* aqueous extract have been used. For the synthesis of PtNPs, leaf extracts of *Xanthium strumarium* and *Fumariae herba* have been used. For the synthesis of PdNPs, Neem wood resin extract has been used. The obtained nanoparticles are suitable for optoelectronic, photocatalytic and pharmaceutical applications. The synthesis of metal/metal oxide nanoparticles via "green" approach allows for obtaining nanoparticles with specified sizes and improved morphology. These new "green" technologies can radically reduce environmental pollution and risk to human health.

Author Contributions: Conceptualization, T.T. and L.S.; writing—original draft preparation, T.T., L.S., O.O.; writing—review and editing, L.S., T.T., M.N.; supervision, T.T. All authors have read and agreed to the published version of the manuscript.

Funding: This research was funded by Ministry of Education and Science of Ukraine, grant number 0121U109476.

Institutional Review Board Statement: Not applicable.

Informed Consent Statement: Not applicable.

Data Availability Statement: Not applicable.

Conflicts of Interest: The authors declare no conflict of interest.

References

1. Das, M.; Chatterjee, S. Chapter 11—Green synthesis of metal/metal oxide nanoparticles toward biomedical applications: Boon or bane. In *Micro and Nano Technologies*; Shukla, A.K., Iravani, S., Eds.; Elsevier: Amsterdam, The Netherlands, 2019; pp. 265–301. ISBN 978-0-08-102579-6.
2. Anastas, P.T.; Warner, J.C. *Green Chemistry: Theory and Practice*; Oxford University Press: New York, NY, USA, 1998.
3. Bourne, R.A.; Poliakoff, M. Green chemistry: What is the way forward? *Mendeleev Commun.* **2011**, *21*, 235–238. [CrossRef]
4. Doble, M.; Kruthiventi, A.K. *Green Chemistry and Engineering*; Academic, P., Ed.; Elsevier: Amsterdam, The Netherlands, 2007; ISBN 9780123725325.
5. Vrček, I.V.; Žuntar, I.; Petlevski, R.; Pavičić, I.; Dutour Sikirić, M.; Ćurlin, M.; Goessler, W. Comparison of in vitro toxicity of silver ions and silver nanoparticles on human hepatoma cells. *Environ. Toxicol.* **2016**, *31*, 679–692. [CrossRef]
6. Xie, K.; Wang, J.; Yu, S.; Wang, P.; Sun, C. Tunable electronic properties of free-standing Fe-doped GaN nanowires as high-capacity anode of lithium-ion batteries. *Arab. J. Chem.* **2021**, *14*, 103161. [CrossRef]
7. Fu, L.; Wang, A.; Xie, K.; Zhu, J.; Chen, F.; Wang, H.; Zhang, H.; Su, W.; Wang, Z.; Zhou, C.; et al. Electrochemical detection of silver ions by using sulfur quantum dots modified gold electrode. *Sens. Actuators B Chem.* **2020**, *304*, 127390. [CrossRef]
8. Passeri, D.; Angeloni, L.; Rossi, M. *Magnetic Force Microscopy and Magnetic Nanoparticles: Perspectives and Challenges*; Springer: Hillerød, Denmark, 2021; pp. 285–300.
9. Sifford, J.; Walsh, K.J.; Tong, S.; Bao, G.; Agarwal, G. Indirect magnetic force microscopy. *Nanoscale Adv.* **2019**, *1*, 2348–2355. [CrossRef]
10. Torre, B.; Bertoni, G.; Fragouli, D.; Falqui, A.; Salerno, M.; Diaspro, A.; Cingolani, R.; Athanassiou, A. Magnetic Force Microscopy and Energy Loss Imaging of Superparamagnetic Iron Oxide Nanoparticles. *Sci. Rep.* **2011**, *1*, 202. [CrossRef]
11. Sievers, S.; Braun, K.F.; Eberbeck, D.; Gustafsson, S.; Olsson, E.; Schumacher, H.W.; Siegner, U. Quantitative measurement of the magnetic moment of individual magnetic nanoparticles by magnetic force microscopy. *Small* **2012**, *8*, 2675–2679. [CrossRef]
12. Cordova, G.; Attwood, S.; Gaikwad, R.; Gu, F.; Leonenko, Z. Magnetic force microscopy characterization of superparamagnetic iron oxide nanoparticles (SPIONs). *Nano Biomed. Eng.* **2014**, *6*, 31–39. [CrossRef]
13. Krivcov, A.; Schneider, J.; Junkers, T.; Möbius, H. Magnetic Force Microscopy of in a Polymer Matrix Embedded Single Magnetic Nanoparticles. *Phys. Status Solidi Appl. Mater. Sci.* **2019**, *216*, 1–8. [CrossRef]
14. Liu, J.; Zhang, W.; Li, Y.; Zhu, H.; Qiu, R.; Song, Z.; Wang, Z.; Li, D. Mechanical manipulation of magnetic nanoparticles by magnetic force microscopy. *J. Magn. Magn. Mater.* **2017**, *443*, 184–189. [CrossRef]
15. Angeloni, L.; Passeri, D.; Reggente, M.; Rossi, M.; Mantovani, D.; Lazzaro, L.; Nepi, F.; De Angelis, F.; Barteri, M. Experimental issues in magnetic force microscopy of nanoparticles. *AIP Conf. Proc.* **2015**, *1667*, 020010.
16. Ahluwalia, V.K.; Kidwai, M. *New Trends in GREEN CHEMISTRY*; Kluwer Academic Publishers with Anamaya Publishers: New Delhi, India, 2004; ISBN 978-94-015-7102-9.
17. Warner, J.C.; Cannon, A.S.; Dye, K.M. Green chemistry. *Environ. Impact Assess. Rev.* **2004**, *24*, 775–799. [CrossRef]
18. Sheldon, R.A.; Arends, I.W.C.E.; Hanefeld, U. *Green Chemistry and Catalysis*; Wiley-VCH Verlag GmbH & Co. KGaA: Weinheim, Germany, 2007; ISBN 9783527307159.
19. Dai, L.; Li, Y.; Liu, R.; Si, C.; Ni, Y. Green mussel-inspired lignin magnetic nanoparticles with high adsorptive capacity and environmental friendliness for chromium(III) removal. *Int. J. Biol. Macromol.* **2019**, *132*, 478–486. [CrossRef]
20. Singh, J.; Dutta, T.; Kim, K.H.; Rawat, M.; Samddar, P.; Kumar, P. "Green" synthesis of metals and their oxide nanoparticles: Applications for environmental remediation. *J. Nanobiotechnol.* **2018**, *16*, 1–24. [CrossRef]
21. Thakkar, K.N.; Mhatre, S.S.; Parikh, R.Y. Biological synthesis of metallic nanoparticles. *Nanomed. Nanotechnol. Biol. Med.* **2010**, *6*, 257–262. [CrossRef]

22. Aravind Kumar, J.; Joshua Amarnath, D.; Anuradha Jabasingh, S.; Senthil Kumar, P.; Vijai Anand, K.; Narendrakumar, G.; Karthick Raja Namasivayam, S.; Krithiga, T.; Sunny, S.; Purna Pushkala, S.; et al. One pot Green Synthesis of Nano magnesium oxide-carbon composite: Preparation, characterization and application towards anthracene adsorption. *J. Clean. Prod.* **2019**, *237*, 117691. [CrossRef]
23. Ismail, M.I.M. Green synthesis and characterizations of copper nanoparticles. *Mater. Chem. Phys.* **2020**, *240*, 122283. [CrossRef]
24. Rana, A.; Yadav, K.; Jagadevan, S. A comprehensive review on green synthesis of nature-inspired metal nanoparticles: Mechanism, application and toxicity. *J. Clean. Prod.* **2020**, *272*, 122880. [CrossRef]
25. Abdelraof, M.; Hasanin, M.S.; Farag, M.M.; Ahmed, H.Y. Green synthesis of bacterial cellulose/bioactive glass nanocomposites: Effect of glass nanoparticles on cellulose yield, biocompatibility and antimicrobial activity. *Int. J. Biol. Macromol.* **2019**, *138*, 975–985. [CrossRef]
26. Abisharani, J.M.; Devikala, S.; Kumar, R.D.; Arthanareeswari, M.; Kamaraj, P. Green synthesis of TiO2 Nanoparticles using Cucurbita pepo seeds extract. *Mater. Today Proc.* **2019**, *14*, 302–307. [CrossRef]
27. Akintelu, S.A.; Folorunso, A.S.; Folorunso, F.A.; Oyebamiji, A.K. Green synthesis of copper oxide nanoparticles for biomedical application and environmental remediation. *Heliyon* **2020**, *6*, e04508. [CrossRef]
28. Mironyuk, I.F.; Soltys, L.M.; Tatarchuk, T.R.; Savka, K.O. Methods of Titanium Dioxide Synthesis (Review). *Phys. Chem. Solid State* **2020**, *21*, 462–477. [CrossRef]
29. Mironyuk, I.F.; Soltys, L.M.; Tatarchuk, T.R.; Tsinurchyn, V.I. Ways to Improve the Efficiency of TiO_2-based Photocatalysts (Review). *Phys. Chem. Solid State* **2020**, *21*, 300–311. [CrossRef]
30. Al-Ruqeishi, M.S.; Mohiuddin, T.; Al-Saadi, L.K. Green synthesis of iron oxide nanorods from deciduous Omani mango tree leaves for heavy oil viscosity treatment. *Arab. J. Chem.* **2019**, *12*, 4084–4090. [CrossRef]
31. Arasu, M.V.; Arokiyaraj, S.; Viayaraghavan, P.; Kumar, T.S.J.; Duraipandiyan, V.; Al-Dhabi, N.A.; Kaviyarasu, K. One step green synthesis of larvicidal, and azo dye degrading antibacterial nanoparticles by response surface methodology. *J. Photochem. Photobiol. B Biol.* **2019**, *190*, 154–162. [CrossRef]
32. Bandeira, M.; Giovanela, M.; Roesch-Ely, M.; Devine, D.M.; da Silva Crespo, J. Green synthesis of zinc oxide nanoparticles: A review of the synthesis methodology and mechanism of formation. *Sustain. Chem. Pharm.* **2020**, *15*, 100223. [CrossRef]
33. Ezealisiji, K.M.; Siwe-Noundou, X.; Maduelosi, B.; Nwachukwu, N.; Krause, R.W.M. Green synthesis of zinc oxide nanoparticles using Solanum torvum (L) leaf extract and evaluation of the toxicological profile of the ZnO nanoparticles–hydrogel composite in Wistar albino rats. *Int. Nano Lett.* **2019**, *9*, 99–107. [CrossRef]
34. Muthukumaran, M.; Dhinagaran, G.; Venkatachalam, K.; Sagadevan, S.; Gunasekaran, S.; Podder, J.; Mohammad, F.; Shahid, M.M.; Oh, W.C. Green synthesis of cuprous oxide nanoparticles for environmental remediation and enhanced visible-light photocatalytic activity. *Optik* **2020**, *214*, 164849. [CrossRef]
35. Sumesh, K.R.; Kanthavel, K. Green Synthesis of Aluminium Oxide Nanoparticles and its Applications in Mechanical and Thermal Stability of Hybrid Natural Composites. *J. Polym. Environ.* **2019**, *27*, 2189–2200. [CrossRef]
36. Suresh, S.; Ilakiya, R.; Kalaiyan, G.; Thambidurai, S.; Kannan, P.; Prabu, K.M.; Suresh, N.; Jothilakshmi, R.; Karthick Kumar, S.; Kandasamy, M. Green Synthesis of Copper Oxide Nanostructures using Cynodon dactylon and Cyperus rotundus Grass Extracts for Antibacterial Applications. *Ceram. Int.* **2020**, *46*, 12525–12537. [CrossRef]
37. Salem, S.S.; Fouda, A. Green Synthesis of Metallic Nanoparticles and Their Prospective Biotechnological Applications: An Overview. *Biol. Trace Elem. Res.* **2021**, *199*, 344–370. [CrossRef]
38. Singh, A.; Gautam, P.K.; Verma, A.; Singh, V.; Shivapriya, P.M.; Shivalkar, S.; Sahoo, A.K.; Samanta, S.K. Green synthesis of metallic nanoparticles as effective alternatives to treat antibiotics resistant bacterial infections: A review. *Biotechnol. Rep.* **2020**, *25*, e00427. [CrossRef]
39. Chen, L.; Batjikh, I.; Hurh, J.; Han, Y.; Huo, Y.; Ali, H.; Li, J.F.; Rupa, E.J.; Ahn, J.C.; Mathiyalagan, R.; et al. Green synthesis of zinc oxide nanoparticles from root extract of Scutellaria baicalensis and its photocatalytic degradation activity using methylene blue. *Optik* **2019**, *184*, 324–329. [CrossRef]
40. Jayappa, M.D.; Ramaiah, C.K.; Kumar, M.A.P.; Suresh, D.; Prabhu, A.; Devasya, R.P.; Sheikh, S. Green synthesis of zinc oxide nanoparticles from the leaf, stem and in vitro grown callus of Mussaenda frondosa L.: Characterization and their applications. *Appl. Nanosci.* **2020**, *10*, 3057–3074. [CrossRef]
41. Pillai, A.M.; Sivasankarapillai, V.S.; Rahdar, A.; Joseph, J.; Sadeghfar, F.; Anuf A., R.; Rajesh, K.; Kyzas, G.Z. Green synthesis and characterization of zinc oxide nanoparticles with antibacterial and antifungal activity. *J. Mol. Struct.* **2020**, *1211*, 128107. [CrossRef]
42. Shabaani, M.; Rahaiee, S.; Zare, M.; Jafari, S.M. Green synthesis of ZnO nanoparticles using loquat seed extract; Biological functions and photocatalytic degradation properties. *LWT* **2020**, *134*, 110133. [CrossRef]
43. Da Silva, A.F.V.; Fagundes, A.P.; Macuvele, D.L.P.; de Carvalho, E.F.U.; Durazzo, M.; Padoin, N.; Soares, C.; Riella, H.G. Green synthesis of zirconia nanoparticles based on Euclea natalensis plant extract: Optimization of reaction conditions and evaluation of adsorptive properties. *Colloids Surf. A Physicochem. Eng. Asp.* **2019**, *583*, 123915. [CrossRef]
44. Elemike, E.E.; Onwudiwe, D.C.; Fayemi, O.E.; Botha, T.L. Green synthesis and electrochemistry of Ag, Au, and Ag–Au bimetallic nanoparticles using golden rod (Solidago canadensis) leaf extract. *Appl. Phys. A* **2019**, *125*, 42. [CrossRef]
45. Ghojavand, S.; Madani, M.; Karimi, J. Green Synthesis, Characterization and Antifungal Activity of Silver Nanoparticles Using Stems and Flowers of Felty Germander. *J. Inorg. Organomet. Polym. Mater.* **2020**, *30*, 2987–2997. [CrossRef]

46. Souri, M.; Hoseinpour, V.; Ghaemi, N.; Shakeri, A. Procedure optimization for green synthesis of manganese dioxide nanoparticles by Yucca gloriosa leaf extract. *Int. Nano Lett.* **2019**, *9*, 73–81. [CrossRef]
47. Chandrababu, P.; Cheriyan, S.; Raghavan, R. Aloe vera leaf extract-assisted facile green synthesis of amorphous Fe2O3 for catalytic thermal decomposition of ammonium perchlorate. *J. Therm. Anal. Calorim.* **2020**, *139*, 89–99. [CrossRef]
48. Długosz, O.; Chwastowski, J.; Banach, M. Hawthorn berries extract for the green synthesis of copper and silver nanoparticles. *Chem. Pap.* **2020**, *74*, 239–252. [CrossRef]
49. Dutta, T.; Ghosh, N.N.; Das, M.; Adhikary, R.; Mandal, V.; Chattopadhyay, A.P. Green synthesis of antibacterial and antifungal silver nanoparticles using Citrus limetta peel extract: Experimental and theoretical studies. *J. Environ. Chem. Eng.* **2020**, *8*, 104019. [CrossRef]
50. Lu, J.; Ali, H.; Hurh, J.; Han, Y.; Batjikh, I.; Rupa, E.J.; Anandapadmanaban, G.; Park, J.K.; Yang, D.-C. The assessment of photocatalytic activity of zinc oxide nanoparticles from the roots of Codonopsis lanceolata synthesized by one-pot green synthesis method. *Optik* **2019**, *184*, 82–89. [CrossRef]
51. Luque, P.A.; Nava, O.; Soto-Robles, C.A.; Chinchillas-Chinchillas, M.J.; Garrafa-Galvez, H.E.; Baez-Lopez, Y.A.; Valdez-Núñez, K.P.; Vilchis-Nestor, A.R.; Castro-Beltrán, A. Improved photocatalytic efficiency of SnO2 nanoparticles through green synthesis. *Optik* **2020**, *206*, 164299. [CrossRef]
52. Arya, A.; Mishra, V.; Chundawat, T.S. Green synthesis of silver nanoparticles from green algae (Botryococcus braunii) and its catalytic behavior for the synthesis of benzimidazoles. *Chem. Data Collect.* **2019**, *20*, 100190. [CrossRef]
53. Chellapandian, C.; Ramkumar, B.; Puja, P.; Shanmuganathan, R.; Pugazhendhi, A.; Kumar, P. Gold nanoparticles using red seaweed Gracilaria verrucosa: Green synthesis, characterization and biocompatibility studies. *Process Biochem.* **2019**, *80*, 58–63. [CrossRef]
54. Sathishkumar, R.S.; Sundaramanickam, A.; Srinath, R.; Ramesh, T.; Saranya, K.; Meena, M.; Surya, P. Green synthesis of silver nanoparticles by bloom forming marine microalgae Trichodesmium erythraeum and its applications in antioxidant, drug-resistant bacteria, and cytotoxicity activity. *J. Saudi Chem. Soc.* **2019**, *23*, 1180–1191. [CrossRef]
55. Sharma, D.; Kanchi, S.; Bisetty, K. Biogenic synthesis of nanoparticles: A review. *Arab. J. Chem.* **2019**, *12*, 3576–3600. [CrossRef]
56. Borah, D.; Das, N.; Das, N.; Bhattacharjee, A.; Sarmah, P.; Ghosh, K.; Chandel, M.; Rout, J.; Pandey, P.; Ghosh, N.N.; et al. Alga-mediated facile green synthesis of silver nanoparticles: Photophysical, catalytic and antibacterial activity. *Appl. Organomet. Chem.* **2020**, *34*, e5597. [CrossRef]
57. Clarance, P.; Luvankar, B.; Sales, J.; Khusro, A.; Agastian, P.; Tack, J.-C.; Al Khulaifi, M.M.; AL-Shwaiman, H.A.; Elgorban, A.M.; Syed, A.; et al. Green synthesis and characterization of gold nanoparticles using endophytic fungi Fusarium solani and its in-vitro anticancer and biomedical applications. *Saudi J. Biol. Sci.* **2020**, *27*, 706–712. [CrossRef]
58. Mahanty, S.; Bakshi, M.; Ghosh, S.; Chatterjee, S.; Bhattacharyya, S.; Das, P.; Das, S.; Chaudhuri, P. Green Synthesis of Iron Oxide Nanoparticles Mediated by Filamentous Fungi Isolated from Sundarban Mangrove Ecosystem, India. *Bionanoscience* **2019**, *9*, 637–651. [CrossRef]
59. Chhipa, H. Chapter 5—Mycosynthesis of nanoparticles for smart agricultural practice: A green and eco-friendly approach. In *Micro and Nano Technologies*; Shukla, A.K., Iravani, S., Eds.; Elsevier: Amsterdam, The Netherlands, 2019; pp. 87–109. ISBN 978-0-08-102579-6.
60. Owaid, M.N. Green synthesis of silver nanoparticles by Pleurotus (oyster mushroom) and their bioactivity: Review. *Environ. Nanotechnol. Monit. Manag.* **2019**, *12*, 100256. [CrossRef]
61. Debnath, G.; Das, P.; Saha, A.K. Green Synthesis of Silver Nanoparticles Using Mushroom Extract of Pleurotus giganteus: Characterization, Antimicrobial, and α-Amylase Inhibitory Activity. *Bionanoscience* **2019**, *9*, 611–619. [CrossRef]
62. Bartosiak, M.; Giersz, J.; Jankowski, K. Analytical monitoring of selenium nanoparticles green synthesis using photochemical vapor generation coupled with MIP-OES and UV–Vis spectrophotometry. *Microchem. J.* **2019**, *145*, 1169–1175. [CrossRef]
63. Akçay, F.A.; Avcı, A. Effects of process conditions and yeast extract on the synthesis of selenium nanoparticles by a novel indigenous isolate Bacillus sp. EKT1 and characterization of nanoparticles. *Arch. Microbiol.* **2020**, *202*, 2233–2243. [CrossRef]
64. Sivaraj, A.; Kumar, V.; Sunder, R.; Parthasarathy, K.; Kasivelu, G. Commercial Yeast Extracts Mediated Green Synthesis of Silver Chloride Nanoparticles and their Anti-mycobacterial Activity. *J. Clust. Sci.* **2020**, *31*, 287–291. [CrossRef]
65. Shu, M.; He, F.; Li, Z.; Zhu, X.; Ma, Y.; Zhou, Z.; Yang, Z.; Gao, F.; Zeng, M. Biosynthesis and Antibacterial Activity of Silver Nanoparticles Using Yeast Extract as Reducing and Capping Agents. *Nanoscale Res. Lett.* **2020**, *15*, 14. [CrossRef]
66. Ahmed, T.; Shahid, M.; Noman, M.; Bilal Khan Niazi, M.; Zubair, M.; Almatroudi, A.; Khurshid, M.; Tariq, F.; Mumtaz, R.; Li, B. Bioprospecting a native silver-resistant Bacillus safensis strain for green synthesis and subsequent antibacterial and anticancer activities of silver nanoparticles. *J. Adv. Res.* **2020**, *24*, 475–483. [CrossRef]
67. Baltazar-Encarnación, E.; Escárcega-González, C.E.; Vasto-Anzaldo, X.G.; Cantú-Cárdenas, M.E.; Morones-Ramírez, J.R. Silver Nanoparticles Synthesized through Green Methods Using *Escherichia coli* Top 10 (Ec-Ts) Growth Culture Medium Exhibit Antimicrobial Properties against Nongrowing Bacterial Strains. *J. Nanomater.* **2019**, *2019*, 4637325. [CrossRef]
68. Patil, M.P.; Kang, M.; Niyonizigiye, I.; Singh, A.; Kim, J.-O.; Seo, Y.B.; Kim, G.-D. Extracellular synthesis of gold nanoparticles using the marine bacterium Paracoccus haeundaensis BC74171T and evaluation of their antioxidant activity and antiproliferative effect on normal and cancer cell lines. *Colloids Surf. B Biointerfaces* **2019**, *183*, 110455. [CrossRef]

69. Ibrahim, E.; Zhang, M.; Zhang, Y.; Hossain, A.; Qiu, W.; Chen, Y.; Wang, Y.; Wu, W.; Sun, G.; Li, B. Green-Synthesization of Silver Nanoparticles Using Endophytic Bacteria Isolated from Garlic and Its Antifungal Activity against Wheat Fusarium Head Blight Pathogen Fusarium graminearum. *Nanomater.* **2020**, *10*, 219. [CrossRef]
70. Sajjad, S.; Leghari, S.A.K.; Ryma, N.U.A.; Farooqi, S.A. *Green Synthesis of Metal-Based Nanoparticles and Their Applications*; Scrivener, Publishing LLC: Beverly, MA, USA, 2018; ISBN 9781119418900.
71. Tatarchuk, T.; Liaskovska, M.; Kotsyubynsky, V.; Bououdina, M. Green synthesis of cobalt ferrite nanoparticles using Cydonia oblonga extract: Structural and mössbauer studies. *Mol. Cryst. Liq. Cryst.* **2018**, *672*, 54–66. [CrossRef]
72. Liaskovska, M.; Tatarchuk, T.; Bououdina, M.; Mironyuk, I. Green Synthesis of Magnetic Spinel Nanoparticles. In Proceedings of the 6th International Conference Nanotechnology and Nanomaterials (NANO2018), Kyiv, Ukraine, 27–30 August 2019; Volume 222.
73. Abdel-Aziz, H.M.; Farag, R.S.; Abdel-Gawad, S.A. Carbamazepine Removal from Aqueous Solution by Green Synthesis Zero-Valent Iron/Cu Nanoparticles with Ficus Benjamina Leaves' Extract. *Int. J. Environ. Res.* **2019**, *13*, 843–852. [CrossRef]
74. Abdullah, J.A.A.; Salah Eddine, L.; Abderrhmane, B.; Alonso-González, M.; Guerrero, A.; Romero, A. Green synthesis and characterization of iron oxide nanoparticles by pheonix dactylifera leaf extract and evaluation of their antioxidant activity. *Sustain. Chem. Pharm.* **2020**, *17*, 100280. [CrossRef]
75. Aksu Demirezen, D.; Yıldız, Y.Ş.; Yılmaz, Ş.; Demirezen Yılmaz, D. Green synthesis and characterization of iron oxide nanoparticles using Ficus carica (common fig) dried fruit extract. *J. Biosci. Bioeng.* **2019**, *127*, 241–245. [CrossRef]
76. Li, Y.; Fu, Y.; Zhu, M. Green synthesis of 3D tripyramid TiO2 architectures with assistance of aloe extracts for highly efficient photocatalytic degradation of antibiotic ciprofloxacin. *Appl. Catal. B Environ.* **2020**, *260*, 118149. [CrossRef]
77. Lohrasbi, S.; Kouhbanani, M.A.J.; Beheshtkhoo, N.; Ghasemi, Y.; Amani, A.M.; Taghizadeh, S. Green Synthesis of Iron Nanoparticles Using Plantago major Leaf Extract and Their Application as a Catalyst for the Decolorization of Azo Dye. *Bionanoscience* **2019**, *9*, 317–322. [CrossRef]
78. Seifipour, R.; Nozari, M.; Pishkar, L. Green Synthesis of Silver Nanoparticles using Tragopogon Collinus Leaf Extract and Study of Their Antibacterial Effects. *J. Inorg. Organomet. Polym. Mater.* **2020**, *30*, 2926–2936. [CrossRef]
79. Alijani, H.Q.; Pourseyedi, S.; Torkzadeh Mahani, M.; Khatami, M. Green synthesis of zinc sulfide (ZnS) nanoparticles using Stevia rebaudiana Bertoni and evaluation of its cytotoxic properties. *J. Mol. Struct.* **2019**, *1175*, 214–218. [CrossRef]
80. Bouafia, A.; Laouini, S.E. Green synthesis of iron oxide nanoparticles by aqueous leaves extract of Mentha Pulegium L.: Effect of ferric chloride concentration on the type of product. *Mater. Lett.* **2020**, *265*, 127364. [CrossRef]
81. Chai, H.-Y.; Lam, S.-M.; Sin, J.-C. Green synthesis of magnetic Fe-doped ZnO nanoparticles via Hibiscus rosa-sinensis leaf extracts for boosted photocatalytic, antibacterial and antifungal activities. *Mater. Lett.* **2019**, *242*, 103–106. [CrossRef]
82. Jemilugba, O.T.; Sakho, E.H.M.; Parani, S.; Mavumengwana, V.; Oluwafemi, O.S. Green synthesis of silver nanoparticles using Combretum erythrophyllum leaves and its antibacterial activities. *Colloid Interface Sci. Commun.* **2019**, *31*, 100191. [CrossRef]
83. Cherian, R.S.; Sandeman, S.; Ray, S.; Savina, I.N.; Ashtami, J.; Mohanan, P.V. Green synthesis of Pluronic stabilized reduced graphene oxide: Chemical and biological characterization. *Colloids Surf. B Biointerfaces* **2019**, *179*, 94–106. [CrossRef]
84. Kumar, I.; Mondal, M.; Sakthivel, N. Chapter 3—Green synthesis of phytogenic nanoparticles. In *Micro and Nano Technologies*; Shukla, A.K., Iravani, S., Eds.; Elsevier: Amsterdam, The Netherlands, 2019; pp. 37–73. ISBN 978-0-08-102579-6.
85. Nasrollahzadeh, M.; Atarod, M.; Sajjadi, M.; Sajadi, S.M.; Issaabadi, Z. Chapter 6—Plant-Mediated Green Synthesis of Nanostructures: Mechanisms, Characterization, and Applications. In *An Introduction to Green Nanotechnology*; Sajadi, M.S., Atarod, M., Nasrollahzadeh, M., Isaabadi, Z., Eds.; Elsevier: Amsterdam, The Netherlands, 2019; Volume 28, pp. 199–322. ISBN 1573-4285.
86. Hussain, M.; Raja, N.I.; Iqbal, M.; Aslam, S. Applications of Plant Flavonoids in the Green Synthesis of Colloidal Silver Nanoparticles and Impacts on Human Health. *Iran. J. Sci. Technol. Trans. A Sci.* **2019**, *43*, 1381–1392. [CrossRef]
87. Chandra, H.; Kumari, P.; Bontempi, E.; Yadav, S. Medicinal plants: Treasure trove for green synthesis of metallic nanoparticles and their biomedical applications. *Biocatal. Agric. Biotechnol.* **2020**, *24*, 101518. [CrossRef]
88. Pal, G.; Rai, P.; Pandey, A. Chapter 1—Green synthesis of nanoparticles: A greener approach for a cleaner future. In *Micro and Nano Technologies*; Shukla, A.K., Iravani, S., Eds.; Elsevier: Amsterdam, The Netherlands, 2019; pp. 1–26. ISBN 978-0-08-102579-6.
89. Islam, N.U.; Jalil, K.; Shahid, M.; Muhammad, N.; Rauf, A. Pistacia integerrima gall extract mediated green synthesis of gold nanoparticles and their biological activities. *Arab. J. Chem.* **2019**, *12*, 2310–2319. [CrossRef]
90. Islam, N.U.; Jalil, K.; Shahid, M.; Rauf, A.; Muhammad, N.; Khan, A.; Shah, M.R.; Khan, M.A. Green synthesis and biological activities of gold nanoparticles functionalized with Salix alba. *Arab. J. Chem.* **2019**, *12*, 2914–2925. [CrossRef]
91. Satpathy, S.; Patra, A.; Ahirwar, B.; Hussain, M.D. Process optimization for green synthesis of gold nanoparticles mediated by extract of Hygrophila spinosa T. Anders and their biological applications. *Phys. E Low-Dimens. Syst. Nanostruct.* **2020**, *121*, 113830. [CrossRef]
92. Thangamani, N.; Bhuvaneshwari, N. Green synthesis of gold nanoparticles using Simarouba glauca leaf extract and their biological activity of micro-organism. *Chem. Phys. Lett.* **2019**, *732*, 136587. [CrossRef]
93. Vijaya Kumar, P.; Mary Jelastin Kala, S.; Prakash, K.S. Green synthesis of gold nanoparticles using Croton Caudatus Geisel leaf extract and their biological studies. *Mater. Lett.* **2019**, *236*, 19–22. [CrossRef]
94. Awad, M.A.; Eisa, N.E.; Virk, P.; Hendi, A.A.; Ortashi, K.M.O.O.; Mahgoub, A.S.A.; Elobeid, M.A.; Eissa, F.Z. Green synthesis of gold nanoparticles: Preparation, characterization, cytotoxicity, and anti-bacterial activities. *Mater. Lett.* **2019**, *256*, 126608. [CrossRef]

95. Aadil, K.R.; Pandey, N.; Mussatto, S.I.; Jha, H. Green synthesis of silver nanoparticles using acacia lignin, their cytotoxicity, catalytic, metal ion sensing capability and antibacterial activity. *J. Environ. Chem. Eng.* **2019**, *7*, 103296. [CrossRef]
96. Behravan, M.; Hossein Panahi, A.; Naghizadeh, A.; Ziaee, M.; Mahdavi, R.; Mirzapour, A. Facile green synthesis of silver nanoparticles using Berberis vulgaris leaf and root aqueous extract and its antibacterial activity. *Int. J. Biol. Macromol.* **2019**, *124*, 148–154. [CrossRef]
97. Bhagat, M.; Anand, R.; Datt, R.; Gupta, V.; Arya, S. Green Synthesis of Silver Nanoparticles Using Aqueous Extract of Rosa brunonii Lindl and Their Morphological, Biological and Photocatalytic Characterizations. *J. Inorg. Organomet. Polym. Mater.* **2019**, *29*, 1039–1047. [CrossRef]
98. Das, P.; Ghosal, K.; Jana, N.K.; Mukherjee, A.; Basak, P. Green synthesis and characterization of silver nanoparticles using belladonna mother tincture and its efficacy as a potential antibacterial and anti-inflammatory agent. *Mater. Chem. Phys.* **2019**, *228*, 310–317. [CrossRef]
99. Gavamukulya, Y.; Maina, E.N.; Meroka, A.M.; Madivoli, E.S.; El-Shemy, H.A.; Wamunyokoli, F.; Magoma, G. Green Synthesis and Characterization of Highly Stable Silver Nanoparticles from Ethanolic Extracts of Fruits of Annona muricata. *J. Inorg. Organomet. Polym. Mater.* **2020**, *30*, 1231–1242. [CrossRef]
100. Hashemi, S.F.; Tasharrofi, N.; Saber, M.M. Green synthesis of silver nanoparticles using Teucrium polium leaf extract and assessment of their antitumor effects against MNK45 human gastric cancer cell line. *J. Mol. Struct.* **2020**, *1208*, 127889. [CrossRef]
101. Jayapriya, M.; Dhanasekaran, D.; Arulmozhi, M.; Nandhakumar, E.; Senthilkumar, N.; Sureshkumar, K. Green synthesis of silver nanoparticles using Piper longum catkin extract irradiated by sunlight: Antibacterial and catalytic activity. *Res. Chem. Intermed.* **2019**, *45*, 3617–3631. [CrossRef]
102. Iravani, S. Green synthesis of metal nanoparticles using plants. *Green Chem.* **2011**, *13*, 2638–2650. [CrossRef]
103. Sharmila, G.; Thirumarimurugan, M.; Muthukumaran, C. Green synthesis of ZnO nanoparticles using Tecoma castanifolia leaf extract: Characterization and evaluation of its antioxidant, bactericidal and anticancer activities. *Microchem. J.* **2019**, *145*, 578–587. [CrossRef]
104. Singh, K.; Singh, J.; Rawat, M. Green synthesis of zinc oxide nanoparticles using Punica Granatum leaf extract and its application towards photocatalytic degradation of Coomassie brilliant blue R-250 dye. *SN Appl. Sci.* **2019**, *1*, 624. [CrossRef]
105. Awual, M.R.; Hasan, M.M.; Eldesoky, G.E.; Khaleque, M.A.; Rahman, M.M.; Naushad, M. Facile mercury detection and removal from aqueous media involving ligand impregnated conjugate nanomaterials. *Chem. Eng. J.* **2016**, *290*, 243–251. [CrossRef]
106. Naushad, M.; ALOthman, Z.A.; Awual, M.R.; Alam, M.M.; Eldesoky, G.E. Adsorption kinetics, isotherms, and thermodynamic studies for the adsorption of Pb2+ and Hg2+ metal ions from aqueous medium using Ti(IV) iodovanadate cation exchanger. *Ionics* **2015**, *21*, 2237–2245. [CrossRef]
107. Sharma, G.; Naushad, M. Adsorptive removal of noxious cadmium ions from aqueous medium using activated carbon/zirconium oxide composite: Isotherm and kinetic modelling. *J. Mol. Liq.* **2020**, *310*, 113025. [CrossRef]
108. Muthusaravanan, S.; Sivarajasekar, N.; Vivek, J.S.; Paramasivan, T.; Naushad, M.; Prakashmaran, J.; Gayathri, V.; Al-Duaij, O.K. Phytoremediation of heavy metals: Mechanisms, methods and enhancements. *Environ. Chem. Lett.* **2018**, *16*, 1339–1359. [CrossRef]
109. Karfa, P.; Madhuri, R. Green tiny magnets: An economic and eco-friendly remedy for environmental damage. In *Green Metal Nanoparticles: Synthesis, Characterization and Their Applications*; Wiley-Scrivener: Beverly, MA, USA, 2018; pp. 245–292.
110. Rossi, L.M.; Parize, A.L.; Rubim, J.C. Green Synthesis and Applications of Magnetic Nanoparticles. *Handb. Green Chem.* **2012**, *8*, 61–88.
111. Tatarchuk, T.; Myslin, M.; Lapchuk, I.; Shyichuk, A.; Murthy, A.P.; Gargula, R.; Kurzydło, P.; Bogacz, B.F.; Pędziwiatr, A.T. Magnesium-zinc ferrites as magnetic adsorbents for Cr(VI) and Ni(II) ions removal: Cation distribution and antistructure modeling. *Chemosphere* **2021**, *270*, 129414. [CrossRef]
112. Tatarchuk, T.; Myslin, M.; Lapchuk, I.; Olkhovyy, O.; Danyliuk, N.; Mandzyuk, V. Synthesis, structure and morphology of magnesium ferrite nanoparticles, synthesized via "green" method. *Phys. Chem. Solid State* **2021**, *22*, 195–203. [CrossRef]
113. Abu-Dief, A.M.; Abdel-Fatah, S.M. Development and functionalization of magnetic nanoparticles as powerful and green catalysts for organic synthesis. *Beni-Suef Univ. J. Basic Appl. Sci.* **2018**, *7*, 55–67. [CrossRef]
114. Yew, Y.P.; Shameli, K.; Miyake, M.; Ahmad Khairudin, N.B.B.; Mohamad, S.E.B.; Naiki, T.; Lee, K.X. Green biosynthesis of superparamagnetic magnetite Fe3O4 nanoparticles and biomedical applications in targeted anticancer drug delivery system: A review. *Arab. J. Chem.* **2018**, *13*, 2287–2308. [CrossRef]
115. Israel, L.L.; Galstyan, A.; Holler, E.; Ljubimova, J.Y. Magnetic iron oxide nanoparticles for imaging, targeting and treatment of primary and metastatic tumors of the brain. *J. Control. Release* **2020**, *320*, 45–62. [CrossRef]
116. Bolade, O.P.; Williams, A.B.; Benson, N.U. Green synthesis of iron-based nanomaterials for environmental remediation: A review. *Environ. Nanotechnol. Monit. Manag.* **2020**, *13*, 100279. [CrossRef]
117. Azizi, A. Green Synthesis of Fe3O4 Nanoparticles and Its Application in Preparation of Fe3O4/Cellulose Magnetic Nanocomposite: A Suitable Proposal for Drug Delivery Systems. *J. Inorg. Organomet. Polym. Mater.* **2020**, *30*, 3552–3561. [CrossRef]
118. Bibi, I.; Nazar, N.; Ata, S.; Sultan, M.; Ali, A.; Abbas, A.; Jilani, K.; Kamal, S.; Sarim, F.M.; Khan, M.I.; et al. Green synthesis of iron oxide nanoparticles using pomegranate seeds extract and photocatalytic activity evaluation for the degradation of textile dye. *J. Mater. Res. Technol.* **2019**, *8*, 6115–6124. [CrossRef]

119. Karpagavinayagam, P.; Vedhi, C. Green synthesis of iron oxide nanoparticles using Avicennia marina flower extract. *Vacuum* **2019**, *160*, 286–292. [CrossRef]
120. Sivakami, M.; Renuka, R.; Thilagavathi, T. Green synthesis of magnetic nanoparticles via Cinnamomum verum bark extract for biological application. *J. Environ. Chem. Eng.* **2020**, *8*, 104420.
121. Mondal, P.; Anweshan, A.; Purkait, M.K. Green synthesis and environmental application of iron-based nanomaterials and nanocomposite: A review. *Chemosphere* **2020**, *259*, 127509. [CrossRef]
122. Naz, S.; Islam, M.; Tabassum, S.; Fernandes, N.F.; Carcache de Blanco, E.J.; Zia, M. Green synthesis of hematite (α-Fe2O3) nanoparticles using Rhus punjabensis extract and their biomedical prospect in pathogenic diseases and cancer. *J. Mol. Struct.* **2019**, *1185*, 1–7. [CrossRef]
123. Qu, Z.; Wu, Y.; Zhu, S.; Yu, Y.; Huo, M.; Zhang, L.; Yang, J.; Bian, D.; Wang, Y. Green Synthesis of Magnetic Adsorbent Using Groundwater Treatment Sludge for Tetracycline Adsorption. *Engineering* **2019**, *5*, 880–887. [CrossRef]
124. De Jesús Ruíz-Baltazar, Á.; Reyes-López, S.Y.; de Lourdes Mondragón-Sánchez, M.; Robles-Cortés, A.I.; Pérez, R. Eco-friendly synthesis of Fe3O4 nanoparticles: Evaluation of their catalytic activity in methylene blue degradation by kinetic adsorption models. *Results Phys.* **2019**, *12*, 989–995. [CrossRef]
125. Cai, W.; Guo, M.; Weng, X.; Zhang, W.; Owens, G.; Chen, Z. Modified green synthesis of Fe3O4@SiO2 nanoparticles for pH responsive drug release. *Mater. Sci. Eng. C* **2020**, *112*, 110900. [CrossRef]
126. Pakzad, K.; Alinezhad, H.; Nasrollahzadeh, M. Green synthesis of Ni@Fe3O4 and CuO nanoparticles using Euphorbia maculata extract as photocatalysts for the degradation of organic pollutants under UV-irradiation. *Ceram. Int.* **2019**, *45*, 17173–17182. [CrossRef]
127. Pan, Z.; Lin, Y.; Sarkar, B.; Owens, G.; Chen, Z. Green synthesis of iron nanoparticles using red peanut skin extract: Synthesis mechanism, characterization and effect of conditions on chromium removal. *J. Colloid Interface Sci.* **2020**, *558*, 106–114. [CrossRef]
128. Rahmani, R.; Gharanfoli, M.; Gholamin, M.; Darroudi, M.; Chamani, J.; Sadri, K. Green synthesis of 99mTc-labeled-Fe3O4 nanoparticles using Quince seeds extract and evaluation of their cytotoxicity and biodistribution in rats. *J. Mol. Struct.* **2019**, *1196*, 394–402. [CrossRef]
129. Yi, Y.; Tu, G.; Tsang, P.E.; Xiao, S.; Fang, Z. Green synthesis of iron-based nanoparticles from extracts of Nephrolepis auriculata and applications for Cr(VI) removal. *Mater. Lett.* **2019**, *234*, 388–391. [CrossRef]
130. Venkateswarlu, S.; Kumar, B.N.; Prathima, B.; SubbaRao, Y.; Jyothi, N.V.V. A novel green synthesis of Fe3O4 magnetic nanorods using Punica Granatum rind extract and its application for removal of Pb(II) from aqueous environment. *Arab. J. Chem.* **2019**, *12*, 588–596. [CrossRef]
131. Niraimathee, V.A.; Subha, V.; Ernest Ravindran, R.S.; Renganathan, S. Green synthesis of iron oxide nanoparticles from Mimosa pudica root extract. *Int. J. Environ. Sustain. Dev.* **2016**, *15*, 227–240. [CrossRef]
132. Lunge, S.; Singh, S.; Sinha, A. Magnetic iron oxide (Fe3O4) nanoparticles from tea waste for arsenic removal. *J. Magn. Magn. Mater.* **2014**, *356*, 21–31. [CrossRef]
133. Bahadur, A.; Saeed, A.; Shoaib, M.; Iqbal, S.; Bashir, M.I.; Waqas, M.; Hussain, M.N.; Abbas, N. Eco-friendly synthesis of magnetite (Fe3O4) nanoparticles with tunable size: Dielectric, magnetic, thermal and optical studies. *Mater. Chem. Phys.* **2017**, *198*, 229–235. [CrossRef]
134. Kanagasubbulakshmi, S.; Kadirvelu, K. Green synthesis of Iron oxide nanoparticles using Lagenaria siceraria and evaluation of its Antimicrobial activity. *Def. Life Sci. J.* **2017**, *2*, 422. [CrossRef]
135. Padhi, D.K.; Panigrahi, T.K.; Parida, K.; Singh, S.K.; Mishra, P.M. Green Synthesis of Fe3O4/RGO Nanocomposite with Enhanced Photocatalytic Performance for Cr(VI) Reduction, Phenol Degradation, and Antibacterial Activity. *ACS Sustain. Chem. Eng.* **2017**, *5*, 10551–10562. [CrossRef]
136. Kataria, N.; Garg, V.K. *Green Synthesis of Fe_3O_4 Nanoparticles Loaded Sawdust Carbon for Cadmium (II) Removal from Water: Regeneration and Mechanism*; Elsevier B.V.: Amsterdam, The Netherlands, 2018; Volume 208, ISBN 9198120581.
137. Ahmadian-Fard-Fini, S.; Salavati-Niasari, M.; Ghanbari, D. Hydrothermal green synthesis of magnetic Fe3O4-carbon dots by lemon and grape fruit extracts and as a photoluminescence sensor for detecting of E. coli bacteria. *Spectrochim. Acta Part A Mol. Biomol. Spectrosc.* **2018**, *203*, 481–493. [CrossRef]
138. Nnadozie, E.C.; Ajibade, P.A. Green synthesis and characterization of magnetite (Fe3O4) nanoparticles using Chromolaena odorata root extract for smart nanocomposite. *Mater. Lett.* **2020**, *263*, 127145. [CrossRef]
139. Khatami, M.; Alijani, H.Q.; Fakheri, B.; Mobasseri, M.M.; Heydarpour, M.; Farahani, Z.K.; Khan, A.U. Super-paramagnetic iron oxide nanoparticles (SPIONs): Greener synthesis using Stevia plant and evaluation of its antioxidant properties. *J. Clean. Prod.* **2019**, *208*, 1171–1177. [CrossRef]
140. Moradi, S.; Khodaiyan, F.; Hadi Razavi, S. Green construction of recyclable amino-tannic acid modified magnetic nanoparticles: Application for β-glucosidase immobilization. *Int. J. Biol. Macromol.* **2020**, *154*, 1366–1374. [CrossRef]
141. Karade, V.C.; Dongale, T.D.; Sahoo, S.C.; Kollu, P.; Chougale, A.D.; Patil, P.S.; Patil, P.B. Effect of reaction time on structural and magnetic properties of green-synthesized magnetic nanoparticles. *J. Phys. Chem. Solids* **2018**, *120*, 161–166. [CrossRef]
142. Fatimah, I.; Zunita Pratiwi, E.; Prio Wicaksono, W. Synthesis of magnetic nanoparticles using Parkia speciosa Hassk pod extract and photocatalytic activity for Bromophenol blue degradation. *Egypt. J. Aquat. Res.* **2020**, *46*, 35–40. [CrossRef]

143. Tatarchuk, T.; Naushad, M.; Tomaszewska, J.; Kosobucki, P.; Myslin, M.; Vasylyeva, H.; Ścigalski, P. Adsorption of Sr(II) ions and salicylic acid onto magnetic magnesium-zinc ferrites: Isotherms and kinetic studies. *Environ. Sci. Pollut. Res.* **2020**, *27*, 26681–26693. [CrossRef]
144. Tatarchuk, T.; Al-Najar, B.; Bououdina, M.; Ahmed, M.A.A. Catalytic and Photocatalytic Properties of Oxide Spinels. In *Handbook of Ecomaterials*; Martínez, L., Kharissova, O., Kharisov, B., Eds.; Springer: Cham, Switzerland, 2019; pp. 1701–1750. ISBN 978-3-319-68254-9.
145. Tatarchuk, T.; Shyichuk, A.; Trawczyńska, I.; Yaremiy, I.; Pędziwiatr, A.T.; Kurzydło, P.; Bogacz, B.F.; Gargula, R. Spinel cobalt(II) ferrite-chromites as catalysts for H2O2 decomposition: Synthesis, morphology, cation distribution and antistructure model of active centers formation. *Ceram. Int.* **2020**, *46*, 27517–27530. [CrossRef]
146. Tatarchuk, T.; Shyichuk, A.; Sojka, Z.; Gryboś, J.; Naushad, M.; Kotsyubynsky, V.; Kowalska, M.; Kwiatkowska-Marks, S.; Danyliuk, N. Green synthesis, structure, cations distribution and bonding characteristics of superparamagnetic cobalt-zinc ferrites nanoparticles for Pb(II) adsorption and magnetic hyperthermia applications. *J. Mol. Liq.* **2021**, *328*, 115375. [CrossRef]
147. Diodati, S.; Pandolfo, L.; Caneschi, A.; Gialanella, S.; Gross, S. Green and low temperature synthesis of nanocrystalline transition metal ferrites by simple wet chemistry routes. *Nano Res.* **2014**, *7*, 1027–1042. [CrossRef]
148. Minelli, A.; Dolcet, P.; Diodati, S.; Gardonio, S.; Innocenti, C.; Badocco, D.; Gialanella, S.; Pastore, P.; Pandolfo, L.; Caneschi, A.; et al. Pursuing the stabilisation of crystalline nanostructured magnetic manganites through a green low temperature hydrothermal synthesis. *J. Mater. Chem. C* **2017**, *5*, 3359–3371. [CrossRef]
149. Joulaei, M.; Hedayati, K.; Ghanbari, D. Investigation of magnetic, mechanical and flame retardant properties of polymeric nanocomposites: Green synthesis of MgFe2O4 by lime and orange extracts. *Compos. Part B Eng.* **2019**, *176*, 107345. [CrossRef]
150. Lestari, M.; Taufiq, A.; Hidayat, A. Green synthesis of $CrFe_2O_4$ nanoparticles using *Cucumis sativus* as a natural surfactant. *Mater. Today Proc.* **2021**, *44*, 3221–3224. [CrossRef]
151. Madhukara Naik, M.; Bhojya Naik, H.S.; Nagaraju, G.; Vinuth, M.; Raja Naika, H.; Vinu, K. Green synthesis of zinc ferrite nanoparticles in Limonia acidissima juice: Characterization and their application as photocatalytic and antibacterial activities. *Microchem. J.* **2019**, *146*, 1227–1235. [CrossRef]
152. Madhukara Naik, M.; Bhojya Naik, H.S.; Nagaraju, G.; Vinuth, M.; Vinu, K.; Viswanath, R. Green synthesis of zinc doped cobalt ferrite nanoparticles: Structural, optical, photocatalytic and antibacterial studies. *Nano-Struct. Nano-Objects* **2019**, *19*, 100322. [CrossRef]
153. Mahajan, P.; Sharma, A.; Kaur, B.; Goyal, N.; Gautam, S. Green synthesized (Ocimum sanctum and Allium sativum) Ag-doped cobalt ferrite nanoparticles for antibacterial application. *Vacuum* **2019**, *161*, 389–397. [CrossRef]
154. Moradnia, F.; Taghavi Fardood, S.; Ramazani, A.; Gupta, V.K. Green synthesis of recyclable MgFeCrO4 spinel nanoparticles for rapid photodegradation of direct black 122 dye. *J. Photochem. Photobiol. A Chem.* **2020**, *392*, 112433. [CrossRef]
155. Hosseini Nasab, N.; Safari, J. Synthesis of a wide range of biologically important spiropyrans and spiroacenaphthylenes, using NiFe2O4@SiO2@Melamine magnetic nanoparticles as an efficient, green and reusable nanocatalyst. *J. Mol. Struct.* **2019**, *1193*, 118–124. [CrossRef]
156. Udhaya, P.A.; Meena, M. Albumen Assisted Green Synthesis of NiFe2O4 Nanoparticles and Their Physico-Chemical Properties. *Mater. Today Proc.* **2019**, *9*, 528–534. [CrossRef]
157. Al-Hunaiti, A.; Al-Said, N.; Halawani, L.; Haija, M.A.; Baqaien, R.; Taher, D. Synthesis of magnetic CuFe2O4 nanoparticles as green catalyst for toluene oxidation under solvent-free conditions. *Arab. J. Chem.* **2020**, *13*, 4945–4953. [CrossRef]
158. Routray, K.L.; Saha, S.; Behera, D. Green synthesis approach for nano sized CoFe2O4 through aloe vera mediated sol-gel auto combustion method for high frequency devices. *Mater. Chem. Phys.* **2019**, *224*, 29–35. [CrossRef]
159. Malakootian, M.; Nasiri, A.; Asadipour, A.; Kargar, E. Facile and green synthesis of ZnFe2O4@CMC as a new magnetic nanophotocatalyst for ciprofloxacin degradation from aqueous media. *Process Saf. Environ. Prot.* **2019**, *129*, 138–151. [CrossRef]
160. Fardood, S.T.; Moradnia, F.; Mostafaei, M.; Afshari, Z.; Faramarzi, V.; Ganjkhanlu, S. Biosynthesis of MgFe 2 O 4 magnetic nanoparticles and their application in photodegradation of malachite green dye and kinetic study. *Nanochem Res.* **2019**, *4*, 86–93.
161. Gayathri Manju, B.; Raji, P. Green Synthesis of Nickel–Copper Mixed Ferrite Nanoparticles: Structural, Optical, Magnetic, Electrochemical and Antibacterial Studies. *J. Electron. Mater.* **2019**, *48*, 7710–7720. [CrossRef]
162. Atrak, K.; Ramazani, A.; Taghavi Fardood, S. Eco-friendly synthesis of Mg0.5Ni0.5AlxFe2-xO4 magnetic nanoparticles and study of their photocatalytic activity for degradation of direct blue 129 dye. *J. Photochem. Photobiol. A Chem.* **2019**, *382*, 111942. [CrossRef]
163. Gutiérrez, M.; Martín, C.; Souza, B.E.; Van der Auweraer, M.; Hofkens, J.; Tan, J.-C. Highly luminescent silver-based MOFs: Scalable eco-friendly synthesis paving the way for photonics sensors and electroluminescent devices. *Appl. Mater. Today* **2020**, *21*, 100817. [CrossRef]
164. Chand, K.; Cao, D.; Eldin Fouad, D.; Hussain Shah, A.; Qadeer Dayo, A.; Zhu, K.; Nazim Lakhan, M.; Mehdi, G.; Dong, S. Green synthesis, characterization and photocatalytic application of silver nanoparticles synthesized by various plant extracts. *Arab. J. Chem.* **2020**, *13*, 8248–8261. [CrossRef]
165. Molina, G.A.; Esparza, R.; López-Miranda, J.L.; Hernández-Martínez, A.R.; España-Sánchez, B.L.; Elizalde-Peña, E.A.; Estevez, M. Green synthesis of Ag nanoflowers using Kalanchoe Daigremontiana extract for enhanced photocatalytic and antibacterial activities. *Colloids Surf. B Biointerfaces* **2019**, *180*, 141–149. [CrossRef]

166. Rashmi, B.N.; Harlapur, S.F.; Avinash, B.; Ravikumar, C.R.; Nagaswarupa, H.P.; Anil Kumar, M.R.; Gurushantha, K.; Santosh, M.S. Facile green synthesis of silver oxide nanoparticles and their electrochemical, photocatalytic and biological studies. *Inorg. Chem. Commun.* **2020**, *111*, 107580. [CrossRef]
167. Ravichandran, V.; Vasanthi, S.; Shalini, S.; Shah, S.A.A.; Tripathy, M.; Paliwal, N. Green synthesis, characterization, antibacterial, antioxidant and photocatalytic activity of Parkia speciosa leaves extract mediated silver nanoparticles. *Results Phys.* **2019**, *15*, 102565. [CrossRef]
168. Saha, B.; Kumar, S.; Sengupta, S. Green synthesis of nano silver on TiO2 catalyst for application in oxidation of thiophene. *Chem. Eng. Sci.* **2019**, *199*, 332–341. [CrossRef]
169. Kareem, M.A.; Bello, I.T.; Shittu, H.A.; Awodele, M.K.; Adedokun, O.; Sanusi, Y.K. Green synthesis of silver nanoparticles (AgNPs) for optical and photocatalytic applications: A review. *IOP Conf. Ser. Mater. Sci. Eng.* **2020**, *805*, 12020. [CrossRef]
170. Alkhalaf, M.I.; Hussein, R.H.; Hamza, A. Green synthesis of silver nanoparticles by Nigella sativa extract alleviates diabetic neuropathy through anti-inflammatory and antioxidant effects. *Saudi J. Biol. Sci.* **2020**, *27*, 2410–2419. [CrossRef] [PubMed]
171. Alfuraydi, A.A.; Devanesan, S.; Al-Ansari, M.; AlSalhi, M.S.; Ranjitsingh, A.J. Eco-friendly green synthesis of silver nanoparticles from the sesame oil cake and its potential anticancer and antimicrobial activities. *J. Photochem. Photobiol. B Biol.* **2019**, *192*, 83–89. [CrossRef]
172. Anandan, M.; Poorani, G.; Boomi, P.; Varunkumar, K.; Anand, K.; Chuturgoon, A.A.; Saravanan, M.; Gurumallesh Prabu, H. Green synthesis of anisotropic silver nanoparticles from the aqueous leaf extract of Dodonaea viscosa with their antibacterial and anticancer activities. *Process Biochem.* **2019**, *80*, 80–88. [CrossRef]
173. Femi-Adepoju, A.G.; Dada, A.O.; Otun, K.O.; Adepoju, A.O.; Fatoba, O.P. Green synthesis of silver nanoparticles using terrestrial fern (Gleichenia Pectinata (Willd.) C. Presl.): Characterization and antimicrobial studies. *Heliyon* **2019**, *5*, e01543. [CrossRef]
174. Girón-Vázquez, N.G.; Gómez-Gutiérrez, C.M.; Soto-Robles, C.A.; Nava, O.; Lugo-Medina, E.; Castrejón-Sánchez, V.H.; Vilchis-Nestor, A.R.; Luque, P.A. Study of the effect of Persea americana seed in the green synthesis of silver nanoparticles and their antimicrobial properties. *Results Phys.* **2019**, *13*, 102142. [CrossRef]
175. Hernández-Morales, L.; Espinoza-Gómez, H.; Flores-López, L.Z.; Sotelo-Barrera, E.L.; Núñez-Rivera, A.; Cadena-Nava, R.D.; Alonso-Núñez, G.; Espinoza, K.A. Study of the green synthesis of silver nanoparticles using a natural extract of dark or white Salvia hispanica L. seeds and their antibacterial application. *Appl. Surf. Sci.* **2019**, *489*, 952–961. [CrossRef]
176. Soto, K.M.; Quezada-Cervantes, C.T.; Hernández-Iturriaga, M.; Luna-Bárcenas, G.; Vazquez-Duhalt, R.; Mendoza, S. Fruit peels waste for the green synthesis of silver nanoparticles with antimicrobial activity against foodborne pathogens. *LWT* **2019**, *103*, 293–300. [CrossRef]
177. El-Sherbiny, I.M.; Salih, E. Green Synthesis of Metallic Nanoparticles Using Biopolymers and Plant Extracts. In *Green Metal Nanoparticles*; Kanchiб, S., Ahmed, S., Eds.; Scrivener Publishing LLC: Beverly, MA, USA, 2018; pp. 293–319.
178. Adyani, S.H.; Soleimani, E. Green synthesis of Ag/Fe3O4/RGO nanocomposites by Punica Granatum peel extract: Catalytic activity for reduction of organic pollutants. *Int. J. Hydrogen Energy* **2019**, *44*, 2711–2730. [CrossRef]
179. Ahmed, R.H.; Mustafa, D.E. Green synthesis of silver nanoparticles mediated by traditionally used medicinal plants in Sudan. *Int. Nano Lett.* **2020**, *10*, 1–14. [CrossRef]
180. Ahmed, T.; Noman, M.; Shahid, M.; Niazi, M.B.K.; Hussain, S.; Manzoor, N.; Wang, X.; Li, B. Green synthesis of silver nanoparticles transformed synthetic textile dye into less toxic intermediate molecules through LC-MS analysis and treated the actual wastewater. *Environ. Res.* **2020**, *191*, 110142. [CrossRef] [PubMed]
181. Banasiuk, R.; Krychowiak, M.; Swigon, D.; Tomaszewicz, W.; Michalak, A.; Chylewska, A.; Ziabka, M.; Lapinski, M.; Koscielska, B.; Narajczyk, M.; et al. Carnivorous plants used for green synthesis of silver nanoparticles with broad-spectrum antimicrobial activity. *Arab. J. Chem.* **2020**, *13*, 1415–1428. [CrossRef]
182. Bindhu, M.R.; Umadevi, M.; Esmail, G.A.; Al-Dhabi, N.A.; Arasu, M.V. Green synthesis and characterization of silver nanoparticles from Moringa oleifera flower and assessment of antimicrobial and sensing properties. *J. Photochem. Photobiol. B Biol.* **2020**, *205*, 111836. [CrossRef]
183. Celebioglu, A.; Topuz, F.; Yildiz, Z.I.; Uyar, T. One-step green synthesis of antibacterial silver nanoparticles embedded in electrospun cyclodextrin nanofibers. *Carbohydr. Polym.* **2019**, *207*, 471–479. [CrossRef]
184. Ferreyra Maillard, A.P.V.; Gonçalves, S.; Santos, N.C.; López de Mishima, B.A.; Dalmasso, P.R.; Hollmann, A. Studies on interaction of green silver nanoparticles with whole bacteria by surface characterization techniques. *Biochim. Biophys. Act Biomembr.* **2019**, *1861*, 1086–1092. [CrossRef]
185. Göl, F.; Aygün, A.; Seyrankaya, A.; Gür, T.; Yenikaya, C.; Şen, F. Green synthesis and characterization of Camellia sinensis mediated silver nanoparticles for antibacterial ceramic applications. *Mater. Chem. Phys.* **2020**, *250*, 123037. [CrossRef]
186. Hamedi, S.; Shojaosadati, S.A. Rapid and green synthesis of silver nanoparticles using Diospyros lotus extract: Evaluation of their biological and catalytic activities. *Polyhedron* **2019**, *171*, 172–180. [CrossRef]
187. Aygün, A.; Özdemir, S.; Gülcan, M.; Cellat, K.; Şen, F. Synthesis and characterization of Reishi mushroom-mediated green synthesis of silver nanoparticles for the biochemical applications. *J. Pharm. Biomed. Anal.* **2020**, *178*. [CrossRef] [PubMed]
188. De Aragão, A.P.; de Oliveira, T.M.; Quelemes, P.V.; Perfeito, M.L.G.; Araújo, M.C.; Santiago, J. de A.S.; Cardoso, V.S.; Quaresma, P.; de Souza de Almeida Leite, J.R.; da Silva, D.A. Green synthesis of silver nanoparticles using the seaweed Gracilaria birdiae and their antibacterial activity. *Arab. J. Chem.* **2019**, *12*, 4182–4188. [CrossRef]

189. Khatami, M.; Sharifi, I.; Nobre, M.A.L.; Zafarnia, N.; Aflatoonian, M.R. Waste-grass-mediated green synthesis of silver nanoparticles and evaluation of their anticancer, antifungal and antibacterial activity. *Green Chem. Lett. Rev.* **2018**, *11*, 125–134. [CrossRef]
190. Saha, J.; Begum, A.; Mukherjee, A.; Kumar, S. A novel green synthesis of silver nanoparticles and their catalytic action in reduction of Methylene Blue dye. *Sustain. Environ. Res.* **2017**, *27*, 245–250. [CrossRef]
191. Nouri, A.; Tavakkoli Yaraki, M.; Lajevardi, A.; Rezaei, Z.; Ghorbanpour, M.; Tanzifi, M. Ultrasonic-assisted green synthesis of silver nanoparticles using Mentha aquatica leaf extract for enhanced antibacterial properties and catalytic activity. *Colloids Interface Sci. Commun.* **2020**, *35*, 100252. [CrossRef]
192. Odeniyi, M.A.; Okumah, V.C.; Adebayo-Tayo, B.C.; Odeniyi, O.A. Green synthesis and cream formulations of silver nanoparticles of Nauclea latifolia (African peach) fruit extracts and evaluation of antimicrobial and antioxidant activities. *Sustain. Chem. Pharm.* **2020**, *15*, 100197. [CrossRef]
193. Fu, Y.; Qin, L.; Huang, D.; Zeng, G.; Lai, C.; Li, B.; He, J.; Yi, H.; Zhang, M.; Cheng, M.; et al. Chitosan functionalized activated coke for Au nanoparticles anchoring: Green synthesis and catalytic activities in hydrogenation of nitrophenols and azo dyes. *Appl. Catal. B Environ.* **2019**, *255*, 117740. [CrossRef]
194. Izadiyan, Z.; Shameli, K.; Miyake, M.; Teow, S.-Y.; Peh, S.-C.; Mohamad, S.E.; Mohd Taib, S.H. Green fabrication of biologically active magnetic core-shell Fe3O4/Au nanoparticles and their potential anticancer effect. *Mater. Sci. Eng. C* **2019**, *96*, 51–57. [CrossRef]
195. Senthilkumar, P.; Surendran, L.; Sudhagar, B.; Ranjith Santhosh Kumar, D.S. Facile green synthesis of gold nanoparticles from marine algae Gelidiella acerosa and evaluation of its biological Potential. *SN Appl. Sci.* **2019**, *1*, 284. [CrossRef]
196. Zhou, M.; Yin, J.; Zhao, X.; Fu, Y.; Jin, X.; Liu, X.; Jiao, T. Green synthesis of gold nanoparticles using Sargassum carpophyllum extract and its application in visual detection of melamine. *Colloids Surf. A Physicochem. Eng. Asp.* **2020**, *603*, 125293. [CrossRef]
197. Molnár, Z.; Bódai, V.; Szakacs, G.; Erdélyi, B.; Fogarassy, Z.; Sáfrán, G.; Varga, T.; Kónya, Z.; Tóth-Szeles, E.; Szucs, R.; et al. Green synthesis of gold nanoparticles by thermophilic filamentous fungi. *Sci. Rep.* **2018**, *8*, 1–12. [CrossRef]
198. Manikandakrishnan, M.; Palanisamy, S.; Vinosha, M.; Kalanjiaraja, B.; Mohandoss, S.; Manikandan, R.; Tabarsa, M.; You, S.G.; Prabhu, N.M. Facile green route synthesis of gold nanoparticles using Caulerpa racemosa for biomedical applications. *J. Drug Deliv. Sci. Technol.* **2019**, *54*, 101345. [CrossRef]
199. Shabestarian, H.; Homayouni-Tabrizi, M.; Soltani, M.; Namvar, F.; Azizi, S.; Mohamad, R.; Shabestarian, H. Green synthesis of gold nanoparticles using sumac aqueous extract and their antioxidant activity. *Mater. Res.* **2017**, *20*, 264–270. [CrossRef]
200. Al-Radadi, N.S. Green synthesis of platinum nanoparticles using Saudi's Dates extract and their usage on the cancer cell treatment. *Arab. J. Chem.* **2019**, *12*, 330–349. [CrossRef]
201. Kumar, P.V.; Jelastin Kala, S.M.; Prakash, K.S. Green synthesis derived Pt-nanoparticles using Xanthium strumarium leaf extract and their biological studies. *J. Environ. Chem. Eng.* **2019**, *7*, 103146. [CrossRef]
202. Dobrucka, R.; Romaniuk-Drapała, A.; Kaczmarek, M. Evaluation of biological synthesized platinum nanoparticles using Ononidis radix extract on the cell lung carcinoma A549. *Biomed. Microdevices* **2019**, *21*, 75. [CrossRef] [PubMed]
203. Dobrucka, R. Biofabrication of platinum nanoparticles using Fumariae herba extract and their catalytic properties. *Saudi J. Biol. Sci.* **2019**, *26*, 31–37. [CrossRef] [PubMed]
204. Puja, P.; Kumar, P. A perspective on biogenic synthesis of platinum nanoparticles and their biomedical applications. *Spectrochim. Acta Part A Mol. Biomol. Spectrosc.* **2019**, *211*, 94–99. [CrossRef]
205. Naseer, A.; Ali, A.; Ali, S.; Mahmood, A.; Kusuma, H.S.; Nazir, A.; Yaseen, M.; Khan, M.I.; Ghaffar, A.; Abbas, M.; et al. Biogenic and eco-benign synthesis of platinum nanoparticles (Pt NPs) using plants aqueous extracts and biological derivatives: Environmental, biological and catalytic applications. *J. Mater. Res. Technol.* **2020**, *9*, 9093–9107. [CrossRef]
206. Rashidi, M.; Islami, M.R.; Tikdari, A.M. Green synthesis of Pd nanoparticles supported on modified Nonpareil almond shell using almond hull extract: A beneficial nanocatalyst for convenient reduction of organic dyes. *J. Mater. Sci. Mater. Electron.* **2019**, *30*, 18111–18122. [CrossRef]
207. Gioria, E.; Signorini, C.; Wisniewski, F.; Gutierrez, L. Green synthesis of time-stable palladium nanoparticles using microfluidic devices. *J. Environ. Chem. Eng.* **2020**, *8*, 104096. [CrossRef]
208. Rostami-Vartooni, A.; Rostami, L.; Bagherzadeh, M. Green synthesis of Fe3O4/bentonite-supported Ag and Pd nanoparticles and investigation of their catalytic activities for the reduction of azo dyes. *J. Mater. Sci. Mater. Electron.* **2019**, *30*, 21377–21387. [CrossRef]
209. Wicaksono, W.P.; Kadja, G.T.M.; Amalia, D.; Uyun, L.; Rini, W.P.; Hidayat, A.; Fahmi, R.L.; Nasriyanti, D.; Leun, S.G.V.; Ariyanta, H.A.; et al. A green synthesis of gold–palladium core–shell nanoparticles using orange peel extract through two-step reduction method and its formaldehyde colorimetric sensing performance. *Nano-Struct. Nano-Objects* **2020**, *24*, 100535. [CrossRef]
210. Bathula, C.; Subalakshmi, K.; Kumar, K.A.; Yadav, H.; Ramesh, S.; Shinde, S.; Shrestha, N.K.; Mallikarjuna, K.; Kim, H. Ultrasonically driven green synthesis of palladium nanoparticles by Coleus amboinicus for catalytic reduction and Suzuki-Miyaura reaction. *Colloids Surf. B Biointerfaces* **2020**, *192*, 111026. [CrossRef]
211. Kiani, M.; Rabiee, N.; Bagherzadeh, M.; Ghadiri, A.M.; Fatahi, Y.; Dinarvand, R.; Webster, T.J. High-gravity-assisted green synthesis of palladium nanoparticles: The flowering of nanomedicine. *Nanomed. Nanotechnol. Biol. Med.* **2020**, *30*, 102297. [CrossRef]
212. Gioria, E.; Wisniewski, F.; Gutierrez, L. Microreactors for the continuous and green synthesis of palladium nanoparticles: Enhancement of the catalytic properties. *J. Environ. Chem. Eng.* **2019**, *7*, 103136. [CrossRef]

213. Olajire, A.A.; Mohammed, A.A. Green synthesis of palladium nanoparticles using Ananas comosus leaf extract for solid-phase photocatalytic degradation of low density polyethylene film. *J. Environ. Chem. Eng.* **2019**, *7*, 103270. [CrossRef]
214. Han, Z.; Dong, L.; Zhang, J.; Cui, T.; Chen, S.; Ma, G.; Guo, X.; Wang, L. Green synthesis of palladium nanoparticles using lentinan for catalytic activity and biological applications. *RSC Adv.* **2019**, *9*, 38265–38270. [CrossRef]
215. Celebioglu, A.; Topuz, F.; Uyar, T. Facile and green synthesis of palladium nanoparticles loaded into cyclodextrin nanofibers and their catalytic application in nitroarene hydrogenation. *New J. Chem.* **2019**, *43*, 3146–3152. [CrossRef]
216. Amrutham, S.; Maragoni, V.; Guttena, V. One-step green synthesis of palladium nanoparticles using neem gum (Azadirachta Indica): Characterization, reduction of Rhodamine 6 G dye and free radical scavenging activity. *Appl. Nanosci.* **2020**, *10*, 4505–4511. [CrossRef]